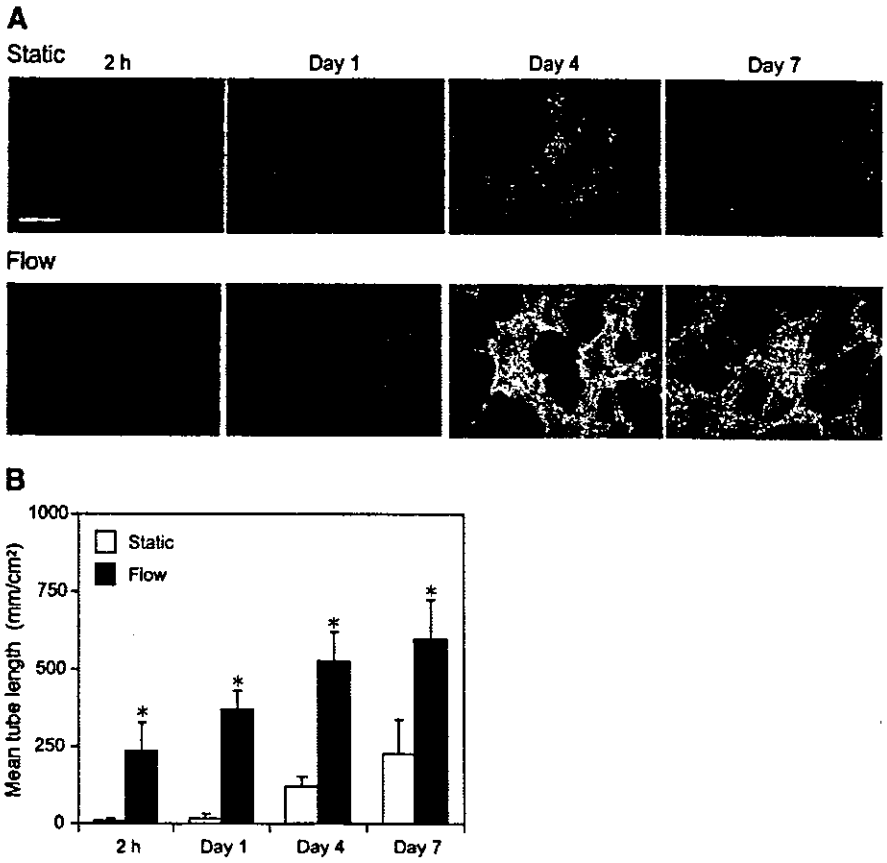

Fig. 5. Tube formation in collagen gel. *A*: representative images captured after incubation for 2 h, and 1, 4, and 7 days. On culture *day 6*, cells that had been incubated under static conditions (Static) or exposed to shear stress (Flow, 0.1–2.5 dyn/cm^2 for 24 h) were seeded onto collagen gels formed with Biocoat Matrigel. Tubelike structures appeared at 4 days in the static EPC cultures but were observed after 1 day in shear-stressed cells and became more extensive with time. The bar indicates 200 μm. *B*: quantification of tube formation. NIH Image was used to determine the total length of the tubelike structures in images captured after incubation for 2 h and 1, 4, and 7 days. Preexposure to shear stress clearly enhanced tubelike structure formation by EPCs. Values are means ± SD of 30 images from 3 separate experiments. *$P < 0.001$ vs. static control.

duced to form capillary-like tubes in fibrin and collagen gels, a monoclonal antibody against VE-cadherin inhibited the formation of capillary tubes, and, when the antibody was added to preformed capillary tubes, it disrupted the capillary network (8). The increase in VE-cadherin induced by shear stress may, therefore, contribute to tube formation and thereby lead to neovascularization.

Vascular ECs can organize into tubular capillary-like structures. An in vitro model in which ECs are cultured in three-dimensional collagen gels in the presence of basic FGF and VEGF has been widely used to study the processes involved in the formation of capillary tubes (43). Use of this model revealed that preconditioning EPCs with shear stress enhanced tube formation. EPCs were exposed to shear stress for 24 h on culture *day 6* and assayed up to 1 wk later. The positive effect of shear stress on tube formation persisted for an entire week. There may be a "memory" effect of 24-h exposure to shear stress that lasts for, at least, 1 wk. The enhanced tube formation appears to be related to shear-stress-induced augmentation of cell growth, VEGF receptor expression, and VE-cadherin expression, although their exact relationships were not assessed in the present study.

In the present study, peripheral blood-derived mononuclear cells that attach to fibronectin-coated dishes, endocytose DiI-acLDL, and bind *Ulex*-lectin were used as EPCs. EPCs have been shown to proliferate, differentiate into mature ECs, form tubelike structures in vitro, and contribute to postnatal neovascularization in vivo (2, 7, 19, 20). Identification of EC precursors, however, has been a source of controversy (35, 36). EPCs were initially isolated from enriched CD34 antigen-positive (CD34$^+$) cells from human peripheral blood (6). CD34 has been used as an EPC marker, and other markers such as AC133 and KDR were subsequently proposed as additional tools to further purify EPCs (16, 44). Recent studies, however, have demonstrated that not only CD34$^+$ cells but also CD34$^-$ cells can function as EPCs; bone marrow- or peripheral blood-derived CD34$^-$ mononuclear cells readily differentiate into EC-like cells in culture and contribute to neovascularization in vivo (17, 38). It has also been shown that EPCs can develop from human peripheral blood CD14-positive monocytes (15, 37). To date, various criteria for EPC selection have been used, including DiI-acLDL(+)-*Ulex*-lectin(+), CD34$^+$ (39), CD34$^+$A133$^+$KDR$^+$ (34), CD34$^-$CD14$^+$ (17), DiI-acLDL(+)vWF$^+$ (29), and CD31$^+$ (21). In this regard, the present data can be said to have been derived from this population of EPCs; peripheral blood derived DiI-acLDL(+)Ulex-lectin(+) adherent mononuclear cells.

The results of this study may have clinical relevance. Application of mechanical stress, such as shear stress or cyclic strain, during the production of artificial vas-

cular grafts from vascular cells grown on a polymer matrix has recently been shown to enhance the development and function of the grafts (31). These engineered grafts exhibit superior mechanical strength and good patency when implanted in miniature swine. More recently, injection of muscles with EPCs isolated from human cord blood was shown to enhance neovascularization in the ischemic legs of nude mice (30). Thus manipulating EPCs by means of mechanical stress may be useful in the development of highly efficient tissue-engineered vessels or for the maturation of EPC cultures outside the body for cell therapy in ischemic vascular diseases.

DISCLOSURES

This work was partly supported by Grants-in-Aid for Scientific Research, for Scientific Research on Priority Areas, and for Special Coordination Funds for Promoting Science and Technology from the Japanese Ministry of Education, Culture, Sports, Science and Technology; by a research grant for cardiovascular diseases from the Japanese Ministry of Health and Welfare; and by Hayashi Memorial Foundation for Female Natural Scientists.

REFERENCES

1. **Akimoto S, Mitsumata M, Sasaguri T, and Yoshida Y.** Laminar shear stress inhibits vascular endothelial cell proliferation by inducing cyclin-dependent kinase inhibitor p21(Sdi1/Cip1/Waf1). *Circ Res* 86: 185–190, 2000.
2. **Akita T, Murohara T, Ikeda H, Sasaki K, Shimada T, Egami K, and Imaizumi T.** Hypoxic preconditioning augments efficacy of human endothelial progenitor cells for therapeutic neovascularization. *Lab Invest* 83: 65–73, 2003.
3. **Ando J, Komatsuda T, Ishikawa C, and Kamiya A.** Fluid shear stress enhanced DNA synthesis in cultured endothelial cells during repair of mechanical denudation. *Biorheology* 27: 675–684, 1990.
4. **Ando J, Nomura H, and Kamiya A.** The effect of fluid shear stress on the migration and proliferation of cultured endothelial cells. *Microvasc Res* 33: 62–70, 1987.
5. **Asahara T, Masuda H, Takahashi T, Kalka C, Pastore C, Silver M, Kearne M, Magner M, and Isner JM.** Bone marrow origin of endothelial progenitor cells responsible for postnatal vasculogenesis in physiological and pathological neovascularization. *Circ Res* 85: 221–228, 1999.
6. **Asahara T, Murohara T, Sullivan A, Silver M, van der Zee R, Li T, Witzenbichler B, Schatteman G, and Isner JM.** Isolation of putative progenitor endothelial cells for angiogenesis. *Science* 275: 964–967, 1997.
7. **Asahara T, Takahashi T, Masuda H, Kalka C, Chen D, Iwaguro H, Inai Y, Silver M, and Isner JM.** VEGF contributes to postnatal neovascularization by mobilizing bone marrow-derived endothelial progenitor cells. *EMBO J* 18: 3964–3972, 1999.
8. **Bach TL, Barsigian C, Chalupowicz DG, Busler D, Yaen CH, Grant DS, and Martinez J.** VE-cadherin mediates endothelial cell capillary tube formation in fibrin and collagen gels. *Exp Cell Res* 238: 324–334, 1998.
9. **Carmeliet P, Lampugnani MG, Moons L, Breviario F, Compernolle V, Bono F, Balconi G, Spagnuolo R, Oostuyse B, Dewerchin M, Zanetti A, Angellilo A, Mattot V, Nuyens D, Lutgens E, Clotman F, de Ruiter MC, Gittenberger-de Groot A, Poelmann R, Lupu F, Herbert JM, Collen D, and Dejana E.** Targeted deficiency or cytosolic truncation of the VE-cadherin gene in mice impairs VEGF-mediated endothelial survival and angiogenesis. *Cell* 98: 147–157, 1999.
10. **Carmeliet P and Luttun A.** The emerging role of the bone marrow-derived stem cells in (therapeutic) angiogenesis. *Thromb Haemost* 86: 289–297, 2001.
11. **Chen KD, Li YS, Kim M, Li S, Yuan S, Chien S, and Shyy JY.** Mechanotransduction in response to shear stress. Roles of receptor tyrosine kinases, integrins, and Shc. *J Biol Chem* 274: 18393–18400, 1999.
12. **Davies PF.** Flow-mediated endothelial mechanotransduction. *Physiol Rev* 75: 519–560, 1995.
13. **Dewey CF.** Effects of fluid flow on living vascular cells. *J Biomech Eng* 106: 31–35, 1984.
14. **Eskin SG, Ives CL, McIntire LV, and Navarro LT.** Response of cultured endothelial cells to steady flow. *Microvasc Res* 28: 87–94, 1984.
15. **Fernandez Pujol B, Lucibello FC, Gehling UM, Lindemann K, Weidner N, Zuzarte ML, Adamkiewicz J, Elsasser HP, Muller R, and Havemann K.** Endothelial-like cells derived from human CD14 positive monocytes. *Differentiation* 65: 287–300, 2000.
16. **Gehling UM, Ergun S, Schumacher U, Wagener C, Pantel K, Otte M, Schuch G, Schafhausen P, Mende T, Kilic N, Kluge K, Schafer B, Hossfeld DK, and Fiedler W.** In vitro differentiation of endothelial cells from AC133-positive progenitor cells. *Blood* 95: 3106–3112, 2000.
17. **Harraz M, Jiao C, Hanlon HD, Hartley RS, and Schatteman GC.** $CD34^-$ blood-derived human endothelial cell progenitors. *Stem Cells* 19: 304–312, 2001.
18. **Hattori K, Dias S, Heissig B, Hackett NR, Lyden D, Tateno M, Hicklin DJ, Zhu Z, Witte L, Crystal RG, Moore MA, and Rafii S.** Vascular endothelial growth factor and angiopoietin-1 stimulate postnatal hematopoiesis by recruitment of vasculogenic and hematopoietic stem cells. *J Exp Med* 193: 1005–1014, 2001.
19. **Kalka C, Masuda H, Takahashi T, Gordon R, Tepper O, Gravereaux E, Pieczek A, Iwaguro H, Hayashi SI, Isner JM, and Asahara T.** Vascular endothelial growth factor(165) gene transfer augments circulating endothelial progenitor cells in human subjects. *Circ Res* 86: 1198–1202, 2000.
20. **Kalka C, Masuda H, Takahashi T, Kalka-Moll WM, Silver M, Kearney M, Li T, Isner JM, and Asahara T.** Transplantation of ex vivo expanded endothelial progenitor cells for therapeutic neovascularization. *Proc Natl Acad Sci USA* 97: 3422–3427, 2000.
21. **Kawamoto A, Tkebuchava T, Yamaguchi J, Nishimura H, Yoon YS, Milliken C, Uchida S, Masuo O, Iwaguro H, Ma H, Hanley A, Silver M, Kearney M, Losordo DW, Isner JM, and Asahara T.** Intramyocardial transplantation of autologous endothelial progenitor cells for therapeutic neovascularization of myocardial ischemia. *Circulation* 107: 461–468, 2003.
22. **Kocher AA, Schuster MD, Szabolcs MJ, Takuma S, Burkhoff D, Wang J, Homma S, Edwards NM, and Itescu S.** Neovascularization of ischemic myocardium by human bone-marrow-derived angioblasts prevents cardiomyocyte apoptosis, reduces remodeling and improves cardiac function. *Nat Med* 7: 430–436, 2001.
23. **Kosaki K, Ando J, Korenaga R, Kurokawa T, and Kamiya A.** Fluid shear stress increases the production of granulocyte-macrophage colony-stimulating factor by endothelial cells via mRNA stabilization. *Circ Res* 82: 794–802, 1998.
24. **Levesque MJ and Nerem RM.** The elongation and orientation of cultured endothelial cells in response to shear stress. *J Biomech Eng* 107: 341–347, 1985.
25. **Levesque MJ, Sprague EA, Schwartz CJ, and Nerem RM.** The influence of shear stress on cultured vascular endothelial cells: the stress response of an anchorage-dependent mammalian cell. *Biotechnol Prog* 5: 1–8, 1989.
26. **Lin Y, Weisdorf DJ, Solovey A, and Hebbel RP.** Origins of circulating endothelial cells and endothelial outgrowth from blood. *J Clin Invest* 105: 71–77, 2000.
27. **Lyden D, Hattori K, Dias S, Costa C, Blaikie P, Butros L, Chadburn A, Heissig B, Marks W, Witte L, Wu Y, Hicklin D, Zhu Z, Hackett NR, Crystal RG, Moore MA, Hajjar KA, Manova K, Benezra R, and Rafii S.** Impaired recruitment of bone-marrow-derived endothelial and hematopoietic precursor cells blocks tumor angiogenesis and growth. *Nat Med* 7: 1194–1201, 2001.

28. **Masuda H, Kawamura K, Tohda K, Shozawa T, Sageshima M, and Kamiya A.** Increase in endothelial cell density before artery enlargement in flow-loaded canine carotid artery. *Arteriosclerosis* 9: 812–823, 1989.
29. **Moore MA, Hattori K, Heissig B, Shieh JH, Dias S, Crystal RG, and Rafii S.** Mobilization of endothelial and hematopoietic stem and progenitor cells by adenovector-mediated elevation of serum levels of SDF-1, VEGF, and angiopoietin-1. *Ann NY Acad Sci* 938: 36–47, 2001.
30. **Murohara T, Ikeda H, Duan J, Shintani S, Sasaki K, Eguchi H, Onitsuka I, Matsui K, and Imaizumi T.** Transplanted cord blood-derived endothelial precursor cells augment postnatal neovascularization. *J Clin Invest* 105: 1527–1536, 2000.
31. **Niklason LE, Gao J, Abbott WM, Hirschi KK, Houser S, Marini R, and Langer R.** Functional arteries grown in vitro. *Science* 284: 489–493, 1999.
32. **Nomura H, Ishikawa C, Komatsuda T, Ando J, and Kamiya A.** A disk-type apparatus for applying fluid shear stress on cultured endothelial cell. *Biorheology* 25: 461–470, 1988.
33. **Noria S, Cowan DB, Gotlieb AI, and Langille BL.** Transient and steady-state effects of shear stress on endothelial cell adherens junctions. *Circ Res* 85: 504–514, 1999.
34. **Peichev M, Naiyer AJ, Pereira D, Zhu Z, Lane WJ, Williams M, Oz MC, Hicklin DJ, Witte L, Moore MA, and Rafii S.** Expression of VEGFR-2 and AC133 by circulating human $CD34^+$ cells identifies a population of functional endothelial precursors. *Blood* 95: 952–958, 2000.
35. **Rabbany SY, Heissig B, Hattori K, and Rafii S.** Molecular pathways regulating mobilization of marrow-derived stem cells for tissue revascularization. *Trends Mol Med* 9: 109–117, 2003.
36. **Rafii S.** Circulating endothelial precursors: mystery, reality, and promise. *J Clin Invest* 105: 17–19, 2000.
37. **Rehman J, Li J, Orschell CM, and March KL.** Peripheral blood "endothelial progenitor cells" are derived from monocyte/macrophages and secrete angiogenic growth factors. *Circulation* 107: 1164–1169, 2003.
38. **Reyes M, Dudek A, Jahagirdar B, Koodie L, Marker PH, and Verfaillie CM.** Origin of endothelial progenitors in human postnatal bone marrow. *J Clin Invest* 109: 337–346, 2002.
39. **Shi Q, Rafii S, Wu MH, Wijelath ES, Yu C, Ishida A, Fujita Y, Kothari S, Mohle R, Sauvage LR, Moore MA, Storb RF, and Hammond WP.** Evidence for circulating bone marrow-derived endothelial cells. *Blood* 92: 362–367, 1998.
40. **Takahashi T, Kalka C, Masuda H, Chen D, Silver M, Kearney M, Magner M, Isner JM, and Asahara T.** Ischemia- and cytokine-induced mobilization of bone marrow-derived endothelial progenitor cells for neovascularization. *Nat Med* 5: 434–438, 1999.
41. **Vittet D, Buchou T, Schweitzer A, Dejana E, and Huber P.** Targeted null-mutation in the vascular endothelial-cadherin gene impairs the organization of vascular-like structures in embryoid bodies. *Proc Natl Acad Sci USA* 94: 6273–6278, 1997.
42. **Wang DM and Tarbell JM.** Modeling interstitial flow in an artery wall allows estimation of wall shear stress on smooth muscle cells. *J Biomech Eng* 117: 358–363, 1995.
43. **Yang S, Graham J, Kahn JW, Schwartz EA, and Gerritsen ME.** Functional roles for PECAM-1 (CD31) and VE-cadherin (CD144) in tube assembly and lumen formation in three-dimensional collagen gels. *Am J Pathol* 155: 887–895, 1999.
44. **Yin AH, Miraglia S, Zanjani ED, Almeida-Porada G, Ogawa M, Leary AG, Olweus J, Kearney J, and Buck DW.** AC133, a novel marker for human hematopoietic stem and progenitor cells. *Blood* 90: 5002–5012, 1997.

Hybrid Cell–Gene Therapy for Pulmonary Hypertension Based on Phagocytosing Action of Endothelial Progenitor Cells

Noritoshi Nagaya, MD; Kenji Kangawa, PhD; Munetake Kanda, MD; Masaaki Uematsu, MD; Takeshi Horio, MD; Naoto Fukuyama, MD; Jun Hino, PhD; Mariko Harada-Shiba, MD; Hiroyuki Okumura, MD; Yasuhiko Tabata, PhD; Naoki Mochizuki, MD; Yoshihide Chiba, MD; Keisuke Nishioka, MD; Kunio Miyatake, MD; Takayuki Asahara, MD; Hiroshi Hara, MD; Hidezo Mori, MD

Background—Circulating endothelial progenitor cells (EPCs) migrate to injured vascular endothelium and differentiate into mature endothelial cells. We investigated whether transplantation of vasodilator gene-transduced EPCs ameliorates monocrotaline (MCT)-induced pulmonary hypertension in rats.

Methods and Results—We obtained EPCs from cultured human umbilical cord blood mononuclear cells and constructed plasmid DNA of adrenomedullin (AM), a potent vasodilator peptide. We used cationic gelatin to produce ionically linked DNA-gelatin complexes. Interestingly, EPCs phagocytosed plasmid DNA-gelatin complexes, which allowed nonviral, highly efficient gene transfer into EPCs. Intravenously administered EPCs were incorporated into the pulmonary vasculature of immunodeficient nude rats given MCT. Transplantation of EPCs alone modestly attenuated MCT-induced pulmonary hypertension (16% decrease in pulmonary vascular resistance). Furthermore, transplantation of AM DNA-transduced EPCs markedly ameliorated pulmonary hypertension in MCT rats (39% decrease in pulmonary vascular resistance). MCT rats transplanted with AM-expressing EPCs had a significantly higher survival rate than those given culture medium or EPCs alone.

Conclusions—Umbilical cord blood–derived EPCs had a phagocytosing action that allowed nonviral, highly efficient gene transfer into EPCs. Transplantation of AM gene-transduced EPCs caused significantly greater improvement in pulmonary hypertension in MCT rats than transplantation of EPCs alone. Thus, a novel hybrid cell–gene therapy based on the phagocytosing action of EPCs may be a new therapeutic strategy for the treatment of pulmonary hypertension. (***Circulation.*** **2003;108:889-895.)**

Key Words: pulmonary heart disease ■ natriuretic peptides ■ gene therapy ■ endothelium

The pulmonary endothelium plays an important role in the regulation of pulmonary vascular tone through the release of vasoactive substances such as nitric oxide, prostacyclin, and adrenomedullin (AM).[1] Dysfunction of the endothelium may play a role in the pathogenesis of pulmonary hypertension, including primary pulmonary hypertension.[2] Thus, pulmonary endothelial cells may be a therapeutic target for the treatment of pulmonary hypertension. Recently, endothelial progenitor cells (EPCs) have been discovered in adult peripheral blood.[3] EPCs are mobilized from bone marrow into the peripheral blood in response to tissue ischemia or traumatic injury, migrate to sites of injured endothelium, and differentiate into mature endothelial cells in situ.[4–6] These findings raise the possibility that transplanted EPCs may serve not only as a tissue-engineering tool to reconstruct the pulmonary vasculature but also as a vehicle for gene delivery to injured pulmonary endothelium.

We prepared biodegradable gelatin that could hold negatively charged protein or plasmid DNA in its positively charged lattice structure.[7,8] We have shown that the gelatin is promptly phagocytosed and then gradually degraded by phagocytes, including macrophages.[9] However, whether EPCs phagocytose ionically linked plasmid DNA-gelatin complexes remains unknown. If this is the case, the phago-

Received December 3, 2002; revision received April 17, 2003; accepted April 18, 2003.

From the Departments of Internal Medicine (N.N., T.H., K.M.) and Perinatology (Y.C.), National Cardiovascular Center, Osaka, Japan; Departments of Biochemistry (K.K., J.H., M.H.-S., H.O.), Cardiac Physiology (M.K., H.M.), and Structural Analysis (N.M.), National Cardiovascular Center Research Institute, Osaka, Japan; Cardiovascular Division (M.U.), Kansai Rosai Hospital, Hyogo, Japan; Department of Physiology (N.F.), Tokai University School of Medicine, Kanagawa, Japan; Department of Biomaterials (Y.T.), Field of Tissue Engineering, Institute for Frontier Medical Sciences, Kyoto University, Kyoto, Japan; Department of Transfusion Medicine (K.N., H.H.), Hyogo College of Medicine, Hyogo, Japan; and Department of Regenerative Medicine (T.A.), Institute of Biomedical Research and Innovation, Kobe, Japan.

Reprint requests to Noritoshi Nagaya, MD, or Hidezo Mori, MD, Department of Internal Medicine, National Cardiovascular Center, 5-7-1 Fujishirodai, Suita, Osaka 565-8565, Japan. E-mail nagayann@hsp.ncvc.go.jp or hidemori@ri.ncvc.go.jp

Circulation is available at http://www.circulationaha.org

DOI: 10.1161/01.CIR.0000079161.56080.22

cytic activity of EPCs would allow nonviral gene transfer into EPCs. Here we provide rationale of a novel hybrid cell–gene therapy for pulmonary hypertension.

AM is a potent vasodilator peptide that was originally isolated from human pheochromocytoma.[1] There are abundant binding sites for AM in the pulmonary vasculature.[10] The plasma AM level increases in proportion to the severity of pulmonary hypertension, and circulating AM is partially metabolized in the lungs.[11] Recently, we have shown that intravenous administration of AM significantly decreases pulmonary vascular resistance in patients with heart failure or primary pulmonary hypertension.[12,13] These findings suggest that AM plays an important role in the regulation of pulmonary vascular tone. Thus, we hypothesized that transplantation of AM DNA-transduced EPCs would improve monocrotaline (MCT)-induced pulmonary hypertension. To test this hypothesis, we investigated whether EPCs phagocytose DNA-gelatin complexes, which would allow nonviral gene transfer into EPCs; whether intravenously administered EPCs are incorporated into the pulmonary vasculature; and whether transplantation of AM DNA-transduced EPCs ameliorates MCT-induced pulmonary hypertension and improves survival in MCT rats.

Methods

Culture of EPCs

Human umbilical cord blood mononuclear cells were plated on fibronectin-coated dishes and cultured in Medium 199 supplemented with 20% FBS, bovine pituitary extract, vascular endothelial growth factor, basic fibroblast growth factor, heparin, and antibiotics, as reported previously.[3,6,14] On days 4 and 8 of culture, nonadherent cells were removed, and medium was replaced. All mothers gave written informed consent, and the study was approved by the ethics committee.

Fluorescent Staining for EPCs

Adherent cells on day 8 of culture were stained by acetylated LDL labeled with DiI (DiI-acLDL, Biomedical Technologies) and fluorescein isothiocyanate (FITC)-labeled lectin from ulex europaeus (Sigma). Double-positive cells for DiI-acLDL and FITC-labeled lectin were identified as EPCs, as reported previously.[15,16]

Flow Cytometry

Adherent cells on day 8 of culture and green fluorescent protein (GFP) gene-transduced cells were analyzed by fluorescence-activated cell sorting (FACS; FACS SCAN flow cytometer, Becton Dickinson). Cells were incubated for 30 minutes at 4°C with phycoerythrin-conjugated mouse monoclonal antibodies against human CD14 (clone M5E2), CD31 (clone L133.1), CD68 (clone Y1/82A), and CD83 (clone HB15e; all from Becton Dickinson) and mouse monoclonal antibodies against human KDR (clone KDR-1, Sigma) and VE-cadherin (clone BV6, Chemicon). Isotype-identical antibodies served as controls.

Preparation of Biodegradable Gelatin and Plasmid DNA

We prepared biodegradable cationic gelatin, as a matrix to hold plasmid DNA, as reported previously.[7] In brief, a gelatin sample with an isoelectric point of 9.0 was isolated from bovine bone collagen. Gelatin microspheres were prepared through the glutaraldehyde cross-linking of gelatin. The microspheres were washed with acetone and distilled water and then freeze-dried. We constructed the pcDNA1.1-CMV vector (Invitrogen) encoding human AM cDNA or GFP cDNA. The gelatin (5 to 30 μm in diameter, 2 mg) was added to plasmid DNA (200 μg/200 μL in PBS, pH 7.4). After 24-hour incubation at 4°C, DNA-gelatin complexes were obtained.

Ex Vivo Gene Transfer Into EPCs

EPCs (5×10^4) were cultured with ionically linked GFP or AM DNA-gelatin complexes (200 μg/2 mg) for 72 hours. To examine DNA localization, AM plasmid DNA was labeled by rhodamine B isothiocyanate (RITC), as reported previously.[8] The nuclei of EPCs were stained by DAPI (Sigma). Immunocytochemistry for AM was performed with a mouse monoclonal antibody against human AM-(46-52). Human AM level in culture medium (n=5) was measured by radioimmunoassay.

Assay for AM

The culture medium and lung tissues were acidified with acetic acid, boiled to inactivate intrinsic proteases, and lyophilized. Human AM levels in culture medium, lung tissues, and plasma were measured with a radioimmunoassay kit (Shionogi).[12]

In Vivo Experimental Protocol

Male immunodeficient (F344/N rnu/rnu) nude rats weighing 100 to 120 g were randomly assigned to receive a subcutaneous injection of 60 mg/kg MCT or 0.9% saline. Seven days after MCT injection, 1×10^6 EPCs, 1×10^6 AM-expressing EPCs, or culture medium (500 μL each) was administered intravenously via the left jugular vein. Sham rats also received intravenous administration of 500 μL of culture medium. We used 1×10^6 cells per rat to obtain maximal effects of transplanted EPCs on the basis of dose-response experiments. This protocol resulted in the creation of 4 groups: MCT rats given EPCs (EPC group, n=8), MCT rats given AM-expressing EPCs (AM-EPC group, n=9), MCT rats given culture medium (control group, n=9), and sham rats given culture medium (sham group, n=8). Human mature pulmonary artery endothelial cells served as control cells.

Hemodynamic studies were performed 3 weeks after MCT injection. A polyethylene catheter was inserted into the right femoral artery. An umbilical vessel catheter was inserted through the right jugular vein into the pulmonary artery. Cardiac output was measured in triplicate by the thermodilution method. Pulmonary vascular resistance was calculated by dividing mean pulmonary arterial pressure by cardiac output.

Immunohistochemical and Immunofluorescence Staining

Immunohistochemistry was performed on paraformaldehyde-fixed, paraffin-embedded 5-μm sections of the lungs. To discern human endothelial cells from rat cells, we used mouse anti-human CD31 (DAKO) and mouse anti-rat CD31 (BD PharMingen) monoclonal antibodies. The sections were sequentially developed for the peroxidase and alkaline phosphatase substrates. Immunofluorescence staining for rat CD31 was performed on frozen sections with mouse anti-rat CD31 monoclonal antibody (BD PharMingen) and RITC-conjugated anti-mouse IgG antibody (DAKO).

Morphometric Analysis of Pulmonary Arteries

We analyzed the medial wall thickness of the pulmonary arteries in the middle region of the right lung (20 muscular arteries/rat, ranging in external diameter from 25 to 50 and from 51 to 100 μm). The medial wall thickness was expressed as follows: % wall thickness=[(medial thickness×2)/external diameter]×100.

Survival Analysis

Seven days after MCT injection, 29 rats received intravenous injection of 1×10^6 EPCs (EPC group, n=10), 1×10^6 AM-expressing EPCs (AM-EPC group, n=10), or culture medium (control group, n=9). Survival was estimated from the date of MCT injection to the death of the rat or 10 weeks after transplantation.

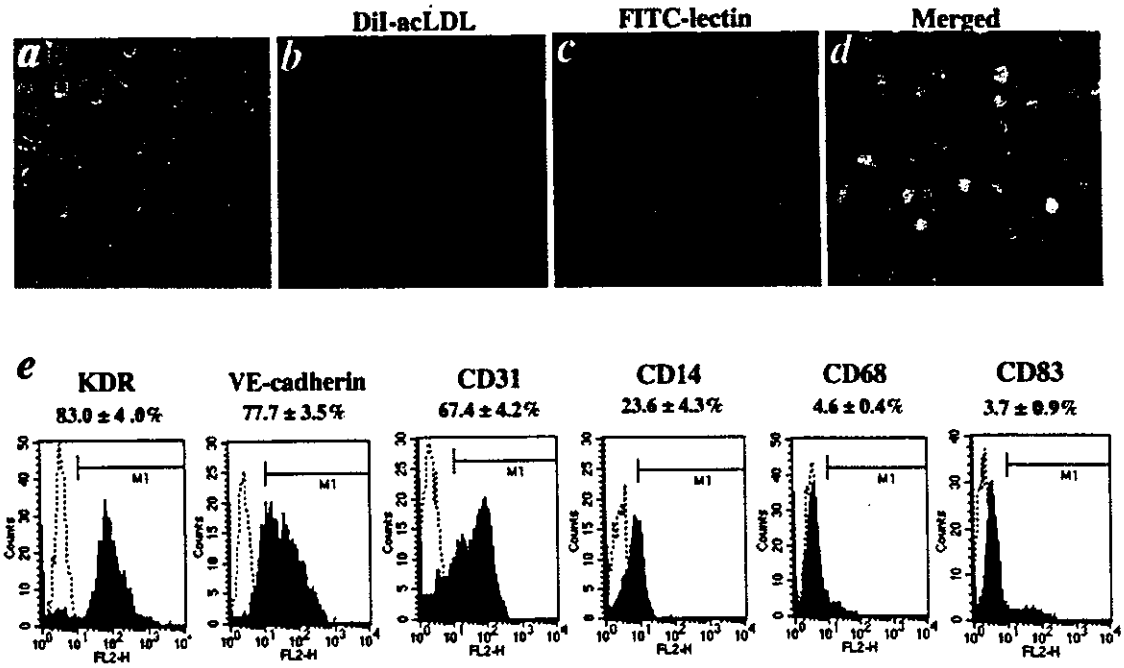

Figure 1. Characterization of EPCs derived from human umbilical cord blood. EPCs exhibited spindle-shaped or cobblestone-like morphology (a) and took up DiI-acLDL and FITC-labeled lectin in same field (b–d). e, Flow cytometric analysis of adherent cells on day 8. Most of adherent cells expressed endothelial lineage markers (KDR, VE-cadherin, and CD31), whereas they were negative for CD68 and CD83.

Statistical Analysis

Data were expressed as mean±SEM. Comparisons of parameters among the 4 groups were made by 1-way ANOVA, followed by the Scheffe multiple comparison test. Comparisons of the time course of parameters between the 2 groups were made by 2-way ANOVA for repeated measures, followed by the Scheffe multiple comparison test. Survival curves were derived by the Kaplan-Meier method and compared with log-rank tests. A probability value <0.05 was considered statistically significant.

Results

EPCs From Human Umbilical Cord Blood

After 8-day culture of mononuclear cells, spindle-shaped or cobblestone-like adherent cells were observed (Figure 1a). Most of the adherent cells were double stained by DiI-acLDL and FITC-labeled lectin (Figure 1b, c, and d). These cells expressed endothelial cell–specific antigens (KDR, VE-cadherin, and CD31; Figure 1e). In contrast, the majority of adherent cells were negative for monocyte/macrophage marker CD68 and dendritic cell marker CD83. Although a small fraction of the adherent cells expressed monocyte marker CD14, this marker has been shown to also be expressed on activated endothelial cells and cultured EPCs.[17] Thus, we confirmed that the major population of the adherent cells were EPCs.

Phagocytosis of DNA-Gelatin Complex by EPCs

EPCs were cultured with GFP DNA-gelatin complexes (Figure 2a). Interestingly, GFP was expressed in EPCs after 72-hour incubation (Figure 2b). Quantitative analyses by FACS confirmed a high incidence (76±3%, n=5) of GFP expression in adherent cells. KDR/GFP double-positive cells made up 70±2% of the adherent cells, whereas CD68/GFP double-positive cells accounted for 2±1% (Figure 2c). Transmission electron microscopy demonstrated that EPCs were phagocytosing DNA-gelatin complexes (Figure 2d). These results suggest that EPCs phagocytose DNA-gelatin complexes in coculture, which allows nonviral, highly efficient gene transfer into EPCs. Unlike gelatin, cationic liposome-mediated transfection efficiency was low (24±3%).

A number of DNA particles labeled by RITC were incorporated into gelatin (Figure 2e). RITC-labeled DNA particles were gradually released from gelatin within EPCs through gelatin degradation (Figure 2f). After 72-hour incubation, RITC-labeled DNA particles released from gelatin were distributed in the cytoplasm of EPCs (Figure 2g). These results suggest the ability of EPCs to take up DNA-gelatin complexes and dissolve the gelatin, freeing the DNA into EPCs. Unlike EPCs, human mature pulmonary artery endothelial cells did not phagocytose DNA-gelatin complexes.

When EPCs were cultured with AM DNA-gelatin complexes, intense immunostaining for AM was observed in EPCs impregnated with AM DNA-gelatin (Figure 3a). After 72-hour incubation, EPCs markedly secreted AM into the culture medium (10-fold increase compared with EPCs alone; Figure 3b). AM overproduction lasted for more than 16 days after gene transfer. AM secretion from EPCs was not influenced by the presence of gelatin (data not shown).

Incorporation of EPCs Into the Pulmonary Vasculature

GFP-expressing EPCs were administered intravenously 7 days after MCT injection. Three days after transplantation,

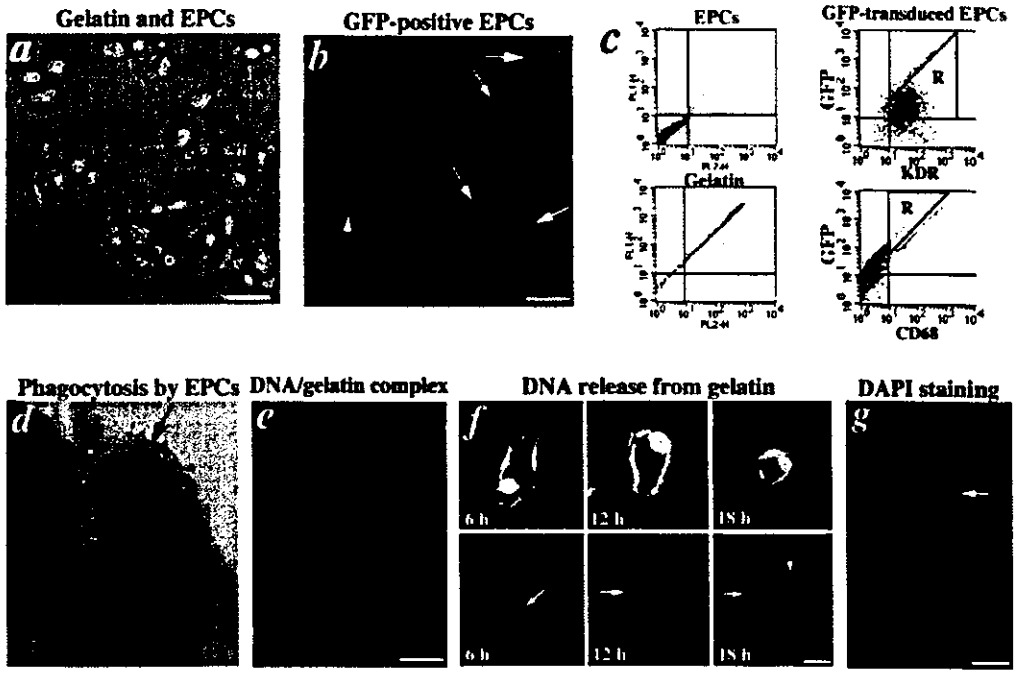

Figure 2. Ex vivo gene transfer into EPCs based on phagocytosing action. a, EPCs were cultured with ionically linked GFP DNA-gelatin complexes. b, GFP was highly expressed in EPCs (arrows) in same field as Figure 2a. c, Flow cytometric analyses of EPCs cultured with GFP DNA-gelatin complexes. Negative controls (EPC isocontrol and gelatin background) are shown in left panels. d, Transmission electron microscopy revealed that EPCs had phagocytosed GFP DNA-gelatin complexes (arrows). e, RITC-labeled DNA particles were incorporated into gelatin. f, RITC-labeled DNA particles (red, arrows) were released from gelatin through its degradation. g, RITC-labeled DNA particles released from gelatin (arrow) were distributed in cytoplasm of EPCs. Nuclei of EPCs were identified by DAPI staining. Scale bars: 10 μm (a and b); 2 μm (d and e); 5 μm (f and g).

GFP-expressing EPCs were incorporated into the walls of pulmonary arterioles in MCT rats and composed pulmonary vasculature (Figure 4a). Transplanted GFP-expressing EPCs were distributed on lung tissues (Figure 4b). AM gene-transduced EPCs were similarly incorporated into the pulmonary vasculature (Figure 4c). Immunohistochemical analyses of rat and human CD31 demonstrated that the transplanted EPCs were of endothelial lineage and comprised a vessel structure similar to rat endothelial cells (Figure 4c). However, transplanted EPCs were rarely distributed to other tissues such as cardiac ventricles, kidneys, aorta, and brain (data not shown).

Effects of Gene-Transduced EPC Transplantation on Pulmonary Hypertension

Pulmonary hypertension developed 3 weeks after MCT injection. Mean pulmonary arterial pressure was not strikingly decreased in the EPC group (−14%) but was significantly lower in the AM-EPC group (−29%) than in the control group (Figure 5a). Pulmonary vascular resistance was significantly lower in both the EPC group (−16%) and the AM-EPC group (−39%) than in the control group (Figure 5b). Importantly, the AM-EPC group showed significantly greater improvement in pulmonary vascular resistance than the EPC group. Right ventricular weight and right ventricular

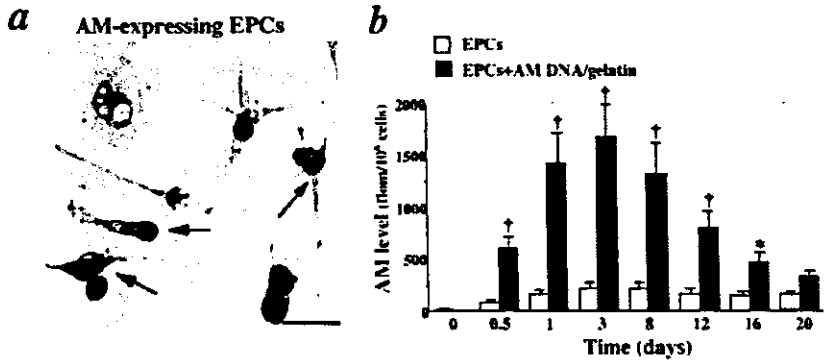

Figure 3. AM gene transfer into EPCs. a, Immunohistochemical analysis of AM in EPCs after gene transfer. Intense immunostaining for AM was observed in EPCs (arrows). Scale bar: 10 μm. b, Time course of AM secretion from EPCs during coculture with AM DNA-gelatin complexes. Data are mean±SEM. *$P<0.05$, †$P<0.001$ vs EPCs.

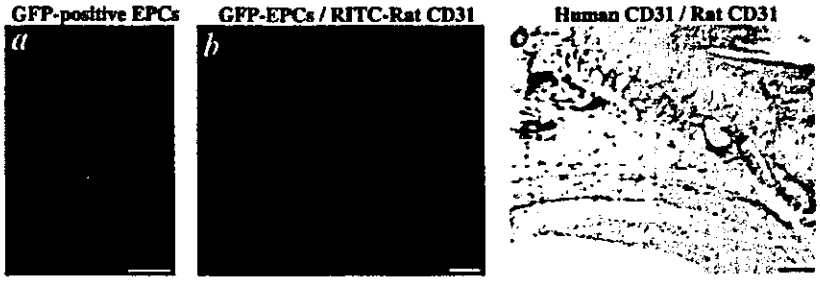

Figure 4. Distribution of EPCs in lungs of MCT rats. a, Intravenously administered GFP-expressing EPCs were incorporated into walls of pulmonary arterioles. b, Transplanted GFP-expressing EPCs were distributed on lung tissues. Pulmonary vasculature was detected by RITC-conjugated anti-rat CD31 (red). c, Immunohistochemistry for human CD31 (peroxidase, brown) and rat CD31 (alkaline phosphatase, pink). Scale bars: 50 μm.

systolic pressure were significantly lower in the AM-EPC group than in the control and EPC groups (Table). AM levels in plasma and lung tissues were significantly higher in the AM-EPC group than in the other groups 2 weeks after transplantation. Unlike EPCs, transplantation of mature pulmonary artery endothelial cells did not significantly influence pulmonary hemodynamics in MCT rats.

Representative photomicrographs showed that hypertrophy of the pulmonary vessel wall after MCT injection was attenuated in both the EPC and AM-EPC groups (Figure 5c). Quantitative analysis also demonstrated a significant increase in percent wall thickness after MCT injection, but this change was markedly attenuated in the AM-EPC group (Figure 5d). Kaplan-Meier survival curves demonstrated that MCT rats transplanted with AM-expressing EPCs (AM-EPC group) had a significantly higher survival rate than those given culture medium (control group) or EPCs alone (EPC group; Figure 5e).

Discussion

In the present study, we present a new concept for cell-based gene delivery into the pulmonary vasculature that consists of 3 processes. First, cationic gelatin is readily complexed with plasmid DNA. Second, EPCs phagocytose ionically linked plasmid DNA-gelatin complexes in coculture, which allows nonviral gene transfer into EPCs with high efficiency. Third, transplanted gene-modified EPCs are incorporated into pulmonary vascular beds in MCT rats. This novel gene delivery system has great advantages over conventional gene therapy: nonviral, noninvasive, and highly efficient gene targeting into the pulmonary vasculature. These benefits may be achieved mainly by the ability of EPCs to phagocytose DNA-gelatin complexes and to migrate to sites of injured endothelium.

Tabata et al[7] and Fukunaka et al[8] demonstrated that gelatin can hold negatively charged protein or plasmid DNA in its positively charged lattice structure. In addition, Tabata et al[9] demonstrated that gelatin is promptly phagocytosed and gradually degraded by macrophages. The present study first demonstrated that EPCs phagocytosed ionically linked DNA-gelatin complexes, dissolved gelatin, and freed the DNA. Surprisingly, the transfection efficiency of this approach was markedly high. FACS analysis demonstrated that EPCs, not monocytes/macrophages, are the main contributors of GFP expression. These findings suggest that the phagocytosing action of EPCs allows nonviral, highly efficient gene transfer into EPCs themselves.

Recently, intravenously administered hematopoietic cells have been shown to be attracted to sites of cerebral injury.[18] Intravenously injected EPCs accumulate in ischemic myocar-

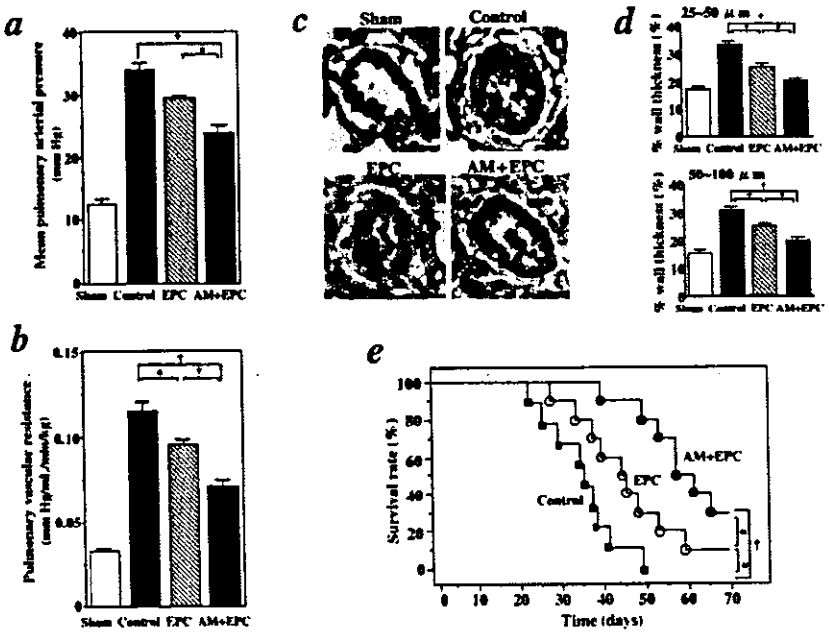

Figure 5. Effects of AM DNA-transduced EPC transplantation on mean pulmonary arterial pressure (a) and pulmonary vascular resistance (b) in MCT rats. c, Representative photomicrographs of peripheral pulmonary arteries in rats. Scale bars, 20 μm. d, Quantitative analysis of percent wall thickness of peripheral pulmonary arteries. e, Kaplan-Meier survival curves of MCT rats transplanted with AM-expressing EPCs (AM-EPC group, ●), EPCs alone (EPC group, ○), or culture medium (control group, □). Data are mean±SEM. *$P<0.05$; †$P<0.001$.

Physiological Profiles of 4 Experimental Groups

	Sham (n=8)	Control (n=9)	EPC (n=8)	AM-EPC (n=9)
Body weight, g	191±4	174±7	181±6	182±6
RV weight, g/kg body weight	0.59±0.02	1.04±0.05	0.91±0.03	0.77±0.04*†
Left ventricular weight, g/kg body weight	2.42±0.03	2.49±0.05	2.46±0.04	2.44±0.09
Heart rate, bpm	398±10	390±11	398±15	387±11
Mean arterial pressure, mm Hg	112±4	100±5	104±3	98±4
RV systolic pressure, mm Hg	32±2	63±3	56±1*	48±2*†
Plasma human AM, fmol/mL	0	0	0.3±0.1*	0.7±0.1*†
Lung human AM, fmol/g tissue	0	0	11.9±0.6*	23.0±2.3*†

Control indicates MCT rats given culture medium; EPC, MCT rats given EPCs; AM-EPC, MCT rats given AM-expressing EPCs; and RV, right ventricular. Data are mean±SEM.
*$P<0.05$ vs control; †$P<0.05$ vs EPC.

dium after acute myocardial infarction.[6] These findings suggest that progenitor cells have the ability to sense injured tissues. In fact, in the present study, intravenously administered GFP-expressing EPCs were incorporated into pulmonary arterioles and capillaries in MCT rats and differentiated mature endothelial cells. MCT injures endothelial cells of small arteries and capillaries in the lungs, resulting in pulmonary hypertension.[19] Taking these findings together, transplanted EPCs may circulate in the blood and attach to injured pulmonary endothelia in MCT rats. Thus, EPCs may serve not only as a vehicle for gene delivery to injured pulmonary endothelia but also as a tissue-engineering tool in restoring intact pulmonary endothelium. Transplantation of EPCs without gene modification slightly but significantly decreased pulmonary vascular resistance in MCT rats. EPCs have been shown to express endothelial nitric oxide synthase and produce nitric oxide.[14] In the present study, we showed that EPCs produce AM even when its gene is not transduced. These results suggest that vasodilator substances secreted from EPCs contribute to improvement in pulmonary hypertension.

We also investigated whether transplantation of gene-modified EPCs causes additional improvement in pulmonary hemodynamics and survival in MCT rats. AM is one of the most potent vasodilators synthesized by vascular endothelial cells.[1] Interestingly, EPCs cultured with AM DNA-gelatin complexes markedly secreted AM protein for more than 16 days. These results suggest relatively long-lasting AM secretion from EPCs. The consequence of this synthesis in MCT rats was a marked decrease in mean pulmonary arterial pressure and pulmonary vascular resistance. Histological examination revealed that transplantation of AM-expressing EPCs inhibited an increase in medial wall thickness of pulmonary arteries. Expectedly, transplantation of AM-expressing EPCs caused significantly greater improvement in pulmonary hypertension and vascular remodeling than transplantation of EPCs alone. Given the known potent vasoprotective effects of AM, such as vasodilation and inhibition of smooth muscle cell proliferation,[1,20] it is interesting to speculate that AM secreted from EPCs may act not only as a circulating factor but also as an autocrine/paracrine factor in the regulation of pulmonary vascular tone and vascular remodeling in MCT rats. Importantly, a single transplantation of AM-expressed EPCs improved survival in MCT rats compared with administration of EPCs alone or culture medium. These results suggest that ex vivo gene transfer into EPCs greatly enhances the therapeutic effects of EPC transplantation. Additional studies are necessary to examine whether repeated administration of EPCs produces an even greater effect than single transplantation.

Conclusions

Human umbilical cord blood–derived EPCs have a phagocytosing action that allows nonviral, highly efficient gene transfer into EPCs. Transplantation of AM DNA-transduced EPCs causes significantly greater improvement in pulmonary hypertension and better survival in MCT rats than transplantation of EPCs alone. Thus, the novel hybrid cell–gene therapy based on the phagocytosing action of EPCs may be a new therapeutic strategy for the treatment of pulmonary hypertension.

Acknowledgments

This work was supported by a grant from the Japan Cardiovascular Research Foundation; HLSRG-RAMT-nano-001 and -RHGTEFB-genome-005, RGCD13C-1 from the Ministry of Health, Labour, and Welfare (MHLW); grants from NEDO; a grant-in-aid for scientific research from the Ministry of Education, Culture, Sports, Science, and Technology (13470154 and 13877114); the Promotion of Fundamental Studies in Health Science of the Organization for Pharmaceutical Safety and Research (OPSR) of Japan; and a grant for Research on Human Genome, Tissue Engineering Food Biotechnology, application of cord blood for blood transplantation and tissue engineering from MHLW. We thank Dr Atsuhiko Kawamoto for his technical assistance.

References

1. Kitamura K, Kangawa K, Kawamoto M, et al. Adrenomedullin: a novel hypotensive peptide isolated from human pheochromocytoma. *Biochem Biophys Res Commun*. 1993;192:553–560.
2. Archer S, Rich S. Primary pulmonary hypertension: a vascular biology and translational research "work in progress." *Circulation*. 2000;102:2781–2791.
3. Asahara T, Murohara T, Sullivan A, et al. Bone marrow origin of endothelial progenitor cells responsible for postnatal vasculogenesis in physiological and pathological neovascularization. *Science*. 1997;275:965–967.

4. Takahashi T, Kalka C, Masuda H, et al. Ischemia- and cytokine-induced mobilization of bone marrow-derived endothelial progenitor cells for neovascularization. *Nat Med*. 1999;5:434–438.
5. Gill M, Dias S, Hattori K, et al. Vascular trauma induces rapid but transient mobilization of VEGFR2(+)AC133(+) endothelial precursor cells. *Circ Res*. 2001;88:167–174.
6. Kawamoto A, Gwon HC, Iwaguro H, et al. Therapeutic potential of ex vivo expanded endothelial progenitor cells for myocardial ischemia. *Circulation*. 2001;103:634–637.
7. Tabata Y, Nagano A, Ikada Y. Biodegradation of hydrogel carrier incorporating fibroblast growth factor. *Tissue Eng*. 1999;5:127–138.
8. Fukunaka Y, Iwanaga K, Morimoto K, et al. Controlled release of plasmid DNA from cationized gelatin hydrogels based on hydrogel degradation. *J Control Release*. 2002;80:333–343.
9. Tabata Y, Ikada Y. Macrophage activation through phagocytosis of muramyl dipeptide encapsulated in gelatin microspheres. *J Pharm Pharmacol*. 1987;39:698–704.
10. Owji AA, Smith DM, Coppock HA, et al. An abundant and specific binding site for the novel vasodilator adrenomedullin in the rat. *Endocrinology*. 1995;136:2127–2134.
11. Yoshibayashi M, Kamiya T, Kitamura K, et al. Plasma levels of adrenomedullin in primary and secondary pulmonary hypertension in patients <20 years of age. *Am J Cardiol*. 1997;79:1556–1558.
12. Nagaya N, Satoh T, Nishikimi T, et al. Hemodynamic, renal and hormonal effects of adrenomedullin infusion in patients with congestive heart failure. *Circulation*. 2000;101:498–503.
13. Nagaya N, Nishikimi T, Uematsu M, et al. Haemodynamic and hormonal effects of adrenomedullin in patients with pulmonary hypertension. *Heart*. 2000;84:653–658.
14. Murohara T, Ikeda H, Duan J, et al. Transplanted cord blood-derived endothelial precursor cells augment postnatal neovascularization. *J Clin Invest*. 2000;105:1527–1536.
15. Kalka C, Masuda H, Takahashi T, et al. Vascular endothelial growth factor (165) gene transfer augments circulating endothelial progenitor cells in human subjects. *Circ Res*. 2000;86:1198–1202.
16. Dimmeler S, Aicher A, Vasa M, et al. HMG-CoA reductase inhibitors (statins) increase endothelial progenitor cells via the PI 3-kinase/Akt pathway. *J Clin Invest*. 2001;108:391–397.
17. Kalka C, Masuda H, Takahashi T, et al. Transplantation of ex vivo expanded endothelial progenitor cells for therapeutic neovascularization. *Proc Natl Acad Sci U S A*. 2000;97:3422–3427.
18. Priller J, Flugel A, Wehner T, et al. Targeting gene-modified hematopoietic cells to the central nervous system: use of green fluorescent protein uncovers microglial engraftment. *Nat Med*. 2001;7:1356–1361.
19. Rosenberg H, Rabinovitch M. Endothelial injury and vascular reactivity in monocrotaline pulmonary hypertension. *Am J Physiol*. 1988;255:H1484–H1491.
20. Horio T, Kohno M, Kano H, et al. Adrenomedullin as a novel antimigration factor of vascular smooth muscle cells. *Circ Res*. 1995;77:660–664.

Engineering the Response to Vascular Injury

Divergent Effects of Deregulated E2F1 Expression on Vascular Smooth Muscle Cells and Endothelial Cells Result in Endothelial Recovery and Inhibition of Neointimal Growth

David A. Goukassian, Raj Kishore, Kevin Krasinski, Christine Dolan, Corinne Luedemann, Young-sup Yoon, Marianne Kearney, Allison Hanley, Hong Ma, Takayuki Asahara, Jeffrey M. Isner,† Douglas W. Losordo

Abstract—Tumor necrosis factor-α (TNF-α) is expressed locally in the vessel wall after angioplasty and induces growth arrest and apoptosis in endothelial cells (ECs), thereby delaying reendothelialization. Prior studies have shown that direct antagonism of TNF-α, using a systemically administered soluble receptor, can enhance endothelial recovery and reduce neointimal thickening. These studies have also shown that downregulation of the transcription factor E2F1 was a key mechanism of TNF's effect on ECs. We now show that Ad-E2F1 overexpression at sites of balloon injury accelerates functional endothelial recovery, consistent with the prior in vitro findings. Moreover these studies also reveal divergent effects of TNF-α and overexpression of E2F1 on ECs versus VSMCs. TNF-α exposure of VSMCs had no affect on proliferation or apoptosis, in contrast to the effect seen in ECs. In Ad-E2F1–transduced VSMCs, however, TNF-α–induced marked apoptosis in contrast to the survival effect seen in ECs. Finally, these studies suggest that differential activation of NF-κB may play a key role in mediating these opposing effects. Nuclear translocation and transcriptional activity of NF-κB was markedly attenuated in Ad-E2F1–transduced VSMCs, whereas it remained active in similarly treated ECs when the cells were exposed to TNF-α. These studies reveal that overexpression of Ad-E2F1 primes VSMCs to TNF-α–induced apoptosis. Furthermore, E2F1 potentiates VSMC death by blocking antiapoptotic signaling pathway through inhibition of NF-κB activation. The divergent responses of VSMCs and ECs to E2F1 overexpression provide unique therapeutic possibilities: simultaneously targeting the cell cycle of two different cell types, within same tissue microenvironment resulting in opposite and biologically complimentary effects. (***Circ Res.* 2003;93:162-169.**)

Key Words: apoptosis ■ vascular smooth muscle cells ■ E2F1 ■ tumor necrosis factor-α ■ nuclear factor-κB

Vascular injury stimulates proliferation and migration of vascular smooth muscle cells (VSMCs), which accumulate in the intima of the injured site. In response to vascular injury, proinflammatory cytokines, such as tumor necrosis factor-α (TNF-α), are produced by activated macrophages as well as by VSMCs themselves.[1] We have previously shown that TNF-α induces apoptosis in proliferating endothelial cells (ECs) via a mechanism involving repression of E2F1 activity. Adenovirus-mediated restoration of E2F1 activity rescued ECs from TNF-α–induced cell cycle arrest and apoptosis.[2] Recently, we also showed that in vivo blockade of TNF-α accelerates functional endothelial recovery and inhibits neointimal lesion formation after balloon angioplasty.[3] These findings indicate that TNF-α expressed locally at sites of balloon arterial injury mediates, at least in part, a delay in endothelial recovery and the associated neointimal lesion formation. These findings also imply that repression of E2F1 activity is a crucial pathway in TNF-α–induced inhibition of endothelial recovery.

To determine if overexpression of E2F1 in vivo would result in restoration of endothelial recovery similar to the documented in vitro effect, we performed an investigation using the rat carotid injury model in which E2F1 was constitutively overexpressed using the same adenoviral vector used for the in vitro studies. These studies revealed acceleration of endothelial recovery consistent with the survival effect shown in vitro. Moreover, these studies also showed attenuation of VSMCs in the neointima. Accordingly,

Original received June 10, 2002; resubmission received December 3, 2002; revised resubmission received May 22, 2003; accepted June 12, 2003.

From the Department of Medicine, Division of Cardiovascular Research (D.A.G., R.K., K.K., C.D., C.L., Y.-s.Y., M.K., A.H., H.M., T.A., J.M.I., D.W.L.), St Elizabeth's Medical Center, Boston, Mass; and the Department of Dermatology (D.A.G.), Boston University School of Medicine, Boston, Mass.

†Deceased.

Correspondence to Douglas W. Losordo, MD, Division of Cardiovascular Medicine, St Elizabeth's Medical Center, 736 Cambridge St, Boston, MA 02135. E-mail douglas.losordo@tufts.edu

Circulation Research is available at http://www.circresaha.org DOI: 10.1161/01.RES.0000082980.94211.3A

we performed a series of in vitro studies to determine the mechanism of the apparently divergent effect of deregulated E2F1 expression on VSMCs and ECs in the setting of TNF-α exposure. In the present study, we show that E2F1 induces VSMCs apoptosis via activation of caspase-dependent pathways. In addition, we also show that E2F1 induces VSMCs apoptosis via downregulation of NF-κB signaling pathway.

Materials and Methods

Rat Carotid Balloon Injury Model

Balloon carotid injury was performed in Sprague-Dawley rats (Charles River Labs, Wilmington, Mass) as previously described.[4] After denuding injury, Ad-E2F1[2] or Ad-β-gal was infused into the isolated carotid segment as described[5] (see online data supplement). All animal protocols were approved by the Institutional Animal Care and Use Committee at the St Elizabeth's Medical Center.

Mouse Carotid Balloon Injury Model

To further examine the role of E2F1 in reendothelialization after balloon injury, we also performed a series of experiments in a mouse model of carotid injury. The mouse carotid injury model, modified in our laboratory from previous methods[6] was used.

Evaluation of Reendothelialization

Reendothelialization was assessed by staining with 0.5% Evans blue dye (Sigma Chemical Co).[4] To verify that the Evans blue stain accurately depicted the presence or absence of endothelium, sections of completely or partially reendothelialized carotid arteries (based on Evans blue appearance) were stained with antibodies to CD31, BS1 Lectin, β-gal, SM-α-Actin, and Factor VIII.[4]

Evaluation of Recovery of Endothelial Function

In order to determine if functional recovery of the endothelium was accelerated by Ad-E2F1 treatment, the production of nitric oxide by excised arterial segments was measured using the Greiss reaction.[4]

Evaluation of Intimal Hyperplasia

Neointimal thickening was evaluated by measuring the total area of neointima in longitudinal sections of elastic-trichrome stained arteries. The area of the media was also measured and the intima/media ratio was calculated.[4]

Evaluation of Proliferation in Injured Arteries

Bromodeoxyuridine (BrdU) (30 mg/kg) (Amersham) was administered by intraperitoneal injection every 12 hours for 48 hours before animal euthanasia (4 injections total). Rat carotid artery segments to be used for immunohistochemistry were perfusion fixed as previously described.[4] BrdU incorporation was evaluated after incubating tissue sections in 2 mol/L HCl for 10 minutes at 37°C to denature DNA.

Culture Conditions and Growth Curves

Human VSMCs, HUVECs, and BAECs were isolated and cultured as previously described.[7] E19P cells (gift from C. Shanahan, Addenbrooke's Hospital, Cambridge, UK) were obtained from explant cultures of embryonic day 19 aorta from Fisher rats. Human recombinant TNF-α was purchased from R&D Systems and, if not otherwise stated, was used at the concentration of 40 ng/mL. This dose was chosen based on our previous studies,[2] which showed efficient induction of apoptosis in ECs within one population doubling (PD) time (usually 12 to 24 hours for ECs). Cell proliferation rates were measured by counting cells at various time points up to 32 hours (usual PD time for VSMCs) using hemocytometer and Coulter counter.

Adenoviral Constructs and Infection

The construct of Ad-β-gal virus used in this study was previously described. Viral stocks of Ad-E2F1, generously supplied by Dr J.R. Nevins, Duke University, Durham, NC, were prepared as previously described. VSMCs and ECs were infected at an MOI of 30 with Ad-E2F1 and Ad-β-gal, if not otherwise stated. Cells were harvested before and at various times after adenoviral infection and processed for studies of proliferation, apoptosis, protein expression, and NF-κB nuclear translocation and transcriptional activity. All adenovirus experiments were done in triplicates and repeated a minimum of three times.

FACS Analysis

Subconfluent VSMCs were synchronized with medium containing 0.5% FBS for 48 hours. Cells were infected with Ad-E2F1 and Ad-β-gal while they were serum-synchronized. Six hours after transduction, cells were released from quiescence by replacing medium with 10% serum containing or not 40 ng/mL TNF-α and harvested at indicated times. Cells were then processed for labeling with FITC-conjugated anti-active caspase 3 antibody (Transduction Laboratories). A second set of similarly treated cells were processed for the detection of apoptosis (annexin V) using commercially available Vibrant Apoptosis Kit (Molecular Probes). Cells were labeled and then fixed according to manufacturer recommendations and analyzed using a FACScan (Becton Dickinson) flow cytometer.

Western Blot Analysis

VSMCs synchronized for 2 days were stimulated with medium containing 10% FBS. Six hours before serum stimulation and TNF-α addition, BAECs and VSMCs were infected with 30 MOI of either Ad-E2F1 or Ad-β-gal. Cells were harvested 0.5 and 2.5 hours after serum/TNF-α stimulation (6.5 and 8.5 hours after AdE2F1 transduction), and E2F1 expression was assessed by Western blot analysis. This experiment was repeated at least two times with similar results. For evaluation of IkB-α degradation, VSMCs and ECs were treated as described above for FACS analysis. At designated time points, cells were lysed and processed for Western blot analysis using anti-IkB-α antibodies (both, 1:200 dilution).[2]

Confocal Microscopy

Six hours before TNF-α exposure, VSMCs were infected with 30 MOI of either Ad-E2F1 or Ad-β-gal. For immunofluorescent studies, control and Ad-E2F1– or Ad-β-gal–transduced VSMCs and HUVECs were serum stimulated in the presence or absence of TNF-α for 30 minutes. Cell monolayers were washed twice with 1×PBS/1%BSA then fixed with ice-cold methanol-acetone (1:1) at −20°C for 10 minutes and air-dried. Next, fixed cells on the chamber slides were reacted with NF-κB (p65) rabbit polyclonal antibody (1:50) for 1 hour at room temperature. After washing with PBS, cells were incubated for 45 minutes with FITC-conjugated secondary antibodies (1:100) (Santa Cruz). Chambers were then removed and slides were mounted with glass cover slips containing 10 μL of Vectashield (Vector, UK).

Transient Transfection Assays

Transient transfection assays, using a luciferase reporter containing the NF-κB *cis*-acting enhancer element (Clontech), were performed to evaluate NF-κB–dependent transcriptional activation. BAECs and E19P cells were co-transfected with NF-κB reporter and control pSVAPAP alkaline phosphatase (AP) with Superfect reagent according to the manufacturer guidelines (QIAGEN). After 16 hours of incubation at 37°C, cells were washed with PBS, trypsinized, pooled, and replated. After 24 hours, cells were serum-starvation synchronized for 48 hours. Six hours before serum stimulation and TNF-α addition, cells were infected with Ad-E2F1 and Ad-β-gal. Cells were harvested at indicated times, lysed with 100 μL reporter lysis buffer (Promega) and processed for measurement of luciferase activity as described. Luciferase activity was normalized relative to the level of (AP) activity produced from co-transfected pSVAPAP plasmid as described previously.

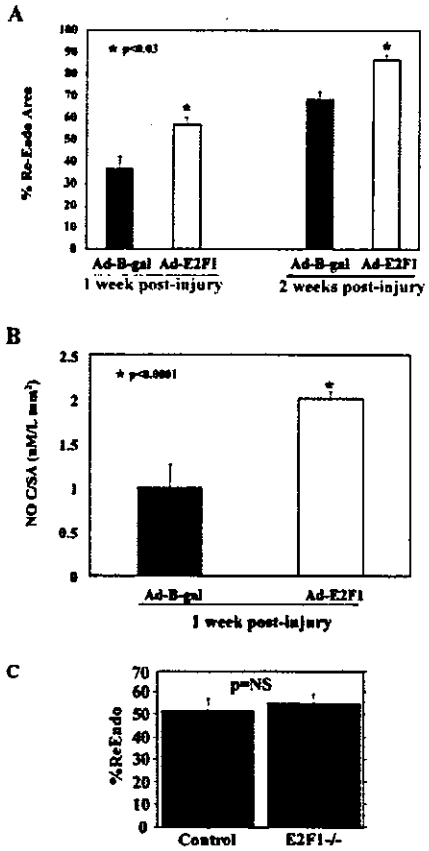

Figure 1. Deregulated E2F1 expression accelerates endothelial recovery after balloon angioplasty. A, Compared with control, Ad-β-gal–transduced arteries, at 1 week and 2 weeks after injury, overexpression of E2F1 accelerates reendothelialization (ReEndo) measured as absolute area reendothelialized. B, Nitric oxide production was measured 1 week after injury. C, Wire injury was performed in 20 E2F1$^{-/-}$ and 20 wild-type 129 mice (genetic background of the E2F1$^{-/-}$) After 7 days, Evans Blue solution was infused, and the arteries were harvested with care taken to identify the injured vessel segment according to anatomic landmarks. Quantification of ReEndo by an investigator blinded to the genotype of the animals revealed no difference in ReEndo in animals with wild-type or null expression of E2F1.

Statistical Analysis

To evaluate statistical significance of differences for cell proliferation and apoptosis studies between experimental groups, ANOVA with Fisher PLSD analysis were performed using StatView statistical program (SAS Inc). Statistical significance was assigned when $P<0.05$.

An expanded Materials and Methods section is available in the online data supplement at http://www.circresaha.org.

Results

Ectopic E2F1 Overexpression Accelerates Functional Endothelial Recovery After Balloon Injury

Quantification of endothelial recovery was performed by measuring the Evans blue–stained region and comparing it to the total area of injury based on standard anatomic landmarks on the excised rat carotid arteries. At both 1 and 2 weeks after injury, endothelial recovery was greater in arteries transduced with Ad-E2F1 versus Ad-β-gal (% injured area reendothelialized at 1 week, E2F1=57.0±3.1% versus β-gal=36.9±5.4%, $P<0.03$; at 2 weeks, E2F1=86.2±2.6% versus β-gal=68.6±3.4%, $P<0.03$) (Figure 1A). The improved anatomic recovery of the endothelium was accompanied by functional endothelial recovery as documented by increased NO production in E2F1 versus control treated arteries: 2.07±0.17 versus 1.02±0.51 nmol/L per mm^2 per 15 minutes; $P<0.0001$ (Figure 1B). The role of E2F1 in endothelial recovery was further explored by comparing endothelial recovery in wild-type (WT) and E2F1$^{-/-}$ mice, revealing no difference in the rate of reendothelialization (Figure 1C). This finding is compatible with functional silencing of E2F1 in WT mice at sites of arterial injury and is consistent with our hypothesis that TNF represses E2F1 activity.

Deregulated E2F1 Expression Reduces Neointimal Thickening and Decreases Neointimal VSMC Proliferation After Balloon Injury

In contrast to the findings of increased endothelial recovery,[2] VSMC proliferation was adversely affected at sites of balloon injury by overexpression of E2F1. The intima/media ratio was reduced significantly in arteries in which E2F1 was overexpressed ($P<0.0057$) (Figure 2A), and this was associated with a decrease in medial cellularity noted at early time points. BrdU labeling revealed evidence of decreased proliferative activity in arteries in which E2F1 was overexpressed (Figure 2B). Thus, in contrast to endothelial cells, in which deregulated E2F1 expression in the setting of TNF-α exposure rescued ECs from apoptosis and cell cycle arrest, in VSMC E2F1 overexpression appeared to have the opposite effect. To further investigate this possibility, a series of in vitro investigations were performed.

E2F1 Cooperates With TNF-α to Inhibit VSMC Cell Cycle

Ad-E2F1 transduction of BAECs and VSMCs led to the time-dependent increase in the level of E2F1 protein that was confirmed by Western blot analysis (Figure 3A). More importantly, exogenous E2F1 protein levels were comparable in both cell types 6.5 and 8.5 hours after transduction. We first examined the effect of TNF-α either alone or in combination with overexpression of E2F1 on the proliferation kinetics of cultured VSMCs. Compared with quiescent cells, serum-stimulated cells showed markedly increased proliferative activity (Figure 3B). TNF-α alone or TNF-α/Ad-β-gal treatment revealed a similar pattern of growth kinetics. In contrast, TNF-α/Ad-E2F1 treatment showed statistically insignificant increases in cell number. Thus compared with all other treatment groups, TNF-α/Ad-E2F1 treatment decreased the number of VSMCs. To assess the distribution of cells at different phases of the cell cycle, FACS analysis of VSMCs stained with propidium iodide was used. No significant difference in the cell cycle distribution of cells was observed in serum-stimulated, TNF-α–, and combined TNF-α/Ad-β-gal–treated cells (Figure 3C). In contrast, compared with TNF-α treatment alone, the number of cells in sub-G_0/G_1 in combined TNF-α/Ad-E2F1–treated cells rose to 8%, a more than 3-fold increase ($P<0.03$). In addition, Ad-E2F1 treatment significantly inhibited entry of cells into G_2/M phase of

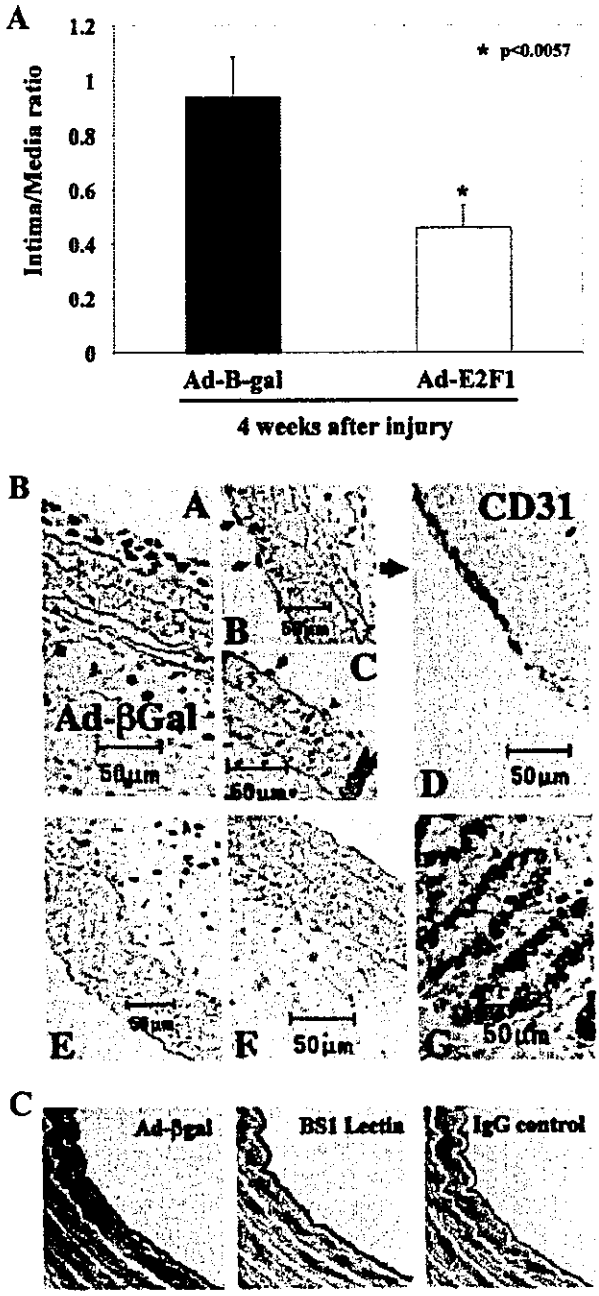

Figure 2. E2F1 inhibits neointimal thickening. A, Computerized planimetric analysis of the total intimal area measured in longitudinally sectioned arteries 4 weeks after balloon injury. Intima/media ratio was calculated by dividing neointimal area by total media area. B, BrdU labeling of proliferating cells in Ad-β-gal– (A) and Ad-E2F1–infected rat arteries 1 week after balloon injury. Foci of proliferating cells were evident in the intima in Ad-β-gal–infected arteries. Ad-E2F1–treated arteries had limited proliferative activity in the VSMC layers (E and F). Proliferating ECs (arrows) were found in the Ad-E2F1–infected arteries (B and C) but could not be identified in Ad-β-gal–infected arteries. Section adjacent to B was stained for CD31 to positively identify endothelial cells (D). Intestines were stained as positive control (G). C, Ad-β-gal and BS1 lectin staining is shown to confirm successful transduction of ECs adjacent to site of balloon injury (see online data supplement).

cell cycle (17% versus 25%, 27.2% and 23% in TNF-α/Ad-E2F1 versus control, TNF-α and TNF-α/Ad-β-gal, respectively; $P<0.05$) (Figure 3C). In addition to regulation of proliferation, the E2F family of transcription factors is also known to regulate pathways leading to apoptosis.[8,9] Accordingly, we examined the rate of apoptosis in VSMCs in which E2F1 was overexpressed in the setting of TNF-α exposure.

Overexpression of E2F1 Induces Apoptosis in TNF-α–Exposed VSMCs

Flow cytometric analysis using antibodies to active caspase 3 revealed a marked increase in apoptosis in VSMCs in which E2F1 was overexpressed. Eighteen hours after treatment, 39±9% of cells treated with TNF-α/Ad-E2F1 were stained positively for active caspase 3 (Figures 4A and 4B). In comparison, only 13±8%, 3.5±2%, and 6±3.8% of serum–, TNF-α–, and TNF-α/Ad-β-gal–treated cells, respectively, were stained positive with active caspase 3 ($P<0.02$, TNF-α/Ad-E2F1 versus all other treatments). These findings suggest that the reduction in cell number documented in vivo and in vitro was not solely due to the inhibition of proliferation but was also the result of E2F1-mediated effects on VSMC viability. These findings were further substantiated by annexin V staining for apoptotic cells. Compared with TNF-α– and TNF-α/Ad-β-gal–treated cells, annexin V positivity was markedly increased in VSMCs that were treated with TNF-α/Ad-E2F1 ($P<0.001$ at 18 hours; Figure 4C). The decrease in VSMC viability resulting from E2F1 overexpression was in sharp contrast to the enhanced survival seen in similarly treated ECs.[2] To better understand the potential mechanisms responsible for this effect, we examined the activity of NF-κB, a transcription factor known to play an essential role in TNF-α–mediated cell survival pathways.[10,11] TUNEL staining for apoptosis in vivo yielded very low rates of positivity in both Ad-E2F1– and Ad-β-gal–treated animals. Others have documented dramatic onset and rapid decrease of apoptosis within the first few hours after balloon injury.[12] In our studies, we concentrated on later time points and could detect in vivo a significant rate of apoptosis. Indeed, given the transient nature of apoptosis in vivo, a significant rate sustained for any period of time would ultimately emaciate the medial layer. This suggests that the effects of TNF-α and E2F1 on proliferation may predominate in vivo.

Overexpression of E2F1 Abrogates NF-κB Nuclear Translocation in TNF-α–Exposed VSMCs

Nuclear translocation of NF-κB (p65) was studied at a single-cell level by confocal microscopy in VSMCs and ECs. In quiescent HUVECs and VSMCs, distribution of NF-κB was predominantly cytoplasmic (Figures 5a and 5f, respectively). Serum stimulation did not alter NF-κB cellular localization in HUVECs, whereas in serum-stimulated VSMCs (30 minutes after serum addition), localization of NF-κB was predominantly nuclear (95±5%) (Figures 5b and 5g). Stimulation of HUVECs and VSMCs with TNF-α for 30 minutes resulted in a marked nuclear translocation of NF-κB in 100±0% of both cell types (Figures 5c and 5h). After combined TNF-α/Ad-E2F1 treatment of HUVECs for 30

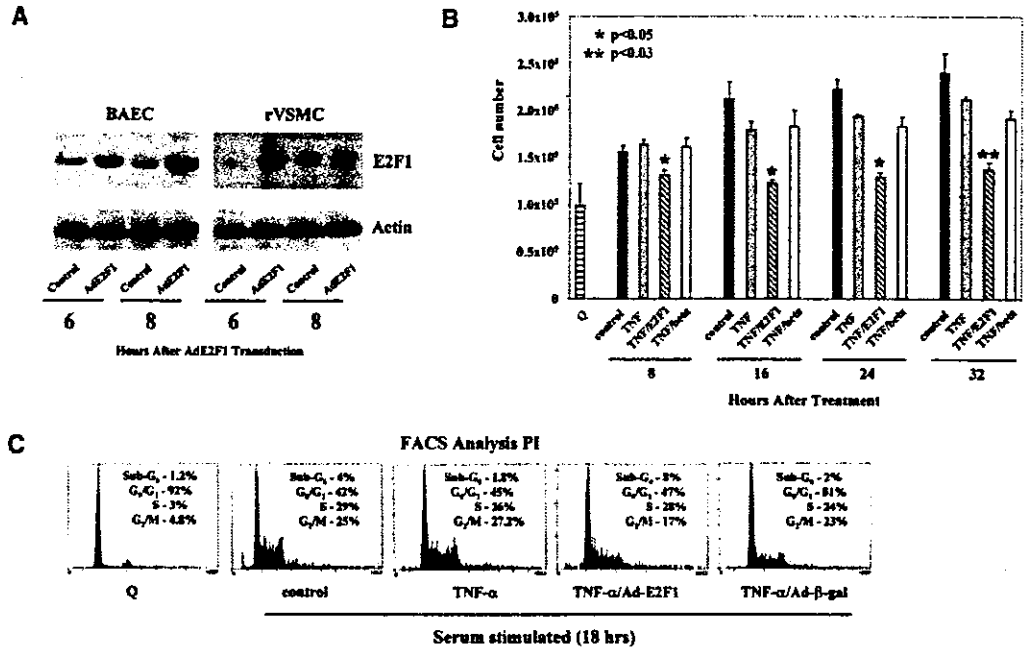

Figure 3. Overexpression of Ad-E2F1 inhibits proliferation and induces apoptosis in VSMCs treated with TNF-α. A, Western blotting shows similar transduction of ECs and VSMCs after infection with Ad-E2F1. B, AdE2F1 overexpression attenuates growth kinetics of cultured VSMCs exposed to TNF-α. Cells were transduced with adenovirus 6 hours before addition of serum±TNF-α. Quiescent cells (horizontal bars) and 8, 16, 24, and 32 hours after serum stimulation (black bars) and addition of TNF-α (40 ng/mL) (gray bars), TNF-α (40 ng/mL)/Ad-E2F1 (30 MOI) (diagonal bars), and TNF-α (40 ng/mL)/Ad-β-gal (30 MOI) (clear bars). C, Before (Q) and 18 hours after serum stimulation, cells were harvested, stained with propidium iodide, and processed for flow cytometric analysis. Representative histograms of FACS analysis are shown revealing an increase in sub-G_1 fraction and a decrease in G_2/M in Ad-E2F1–transduced VSMCs exposed to TNF.

minutes, NF-κB remained translocated to the nucleus in 100% of cells (Figure 5d). In contrast, nuclear translocation of NF-κB was completely abrogated when E2F1 was overexpressed in TNF-α exposed VSMCs (Figure 5i). In both cell types, TNF-α/Ad-β-gal–treated cells manifested similar degrees of NF-κB nuclear translocation to serum only and/or serum/TNF-α–treated cells (Figures 5e and 5j).

Overexpression of E2F1 Inhibits IkB-α Degradation in TNF-α–Exposed VSMCs

IkB-α degradation was studied by Western blot analysis in BAECs versus VSMCs in the setting of combined TNF-α/AdE2F1 treatment. Serum stimulation led to rapid degradation of IkB-α in VSMCs (15 minutes), whereas in serum-stimulated BAECs, IkB-α levels were comparable to levels of quiescent cells (Figure 6). Treatment with TNF-α alone or in combination with Ad-β-gal led to comparable IkB-α degradation in VSMCs, as well as in ECs; however, IkB-α degradation was more prominent in VSMCs. Interestingly, these two cell types responded differently to the combined TNF-α/AdE2F1 treatment. In VSMCs, E2F1 overexpression inhibited IkB-α degradation, thereby preventing NF-κB activation in VSMCs, whereas E2F1 overexpression led to the rapid IkB-α degradation (TNF-α and/or TNF-α/Ad-β-gal treatments) in ECs (Figure 6), suggesting a possible mechanism of divergent effects of E2F1 overexpression in VSMCs versus ECs.

Overexpression of E2F1 Abrogates NF-κB Transcriptional Activity in VSMCs but Remains Intact in ECs

To verify that the alterations in NF-κB translocation were associated with a functional change in NF-κB–mediated transcriptional activity, we performed a series of transient transfection assays using a luciferase reporter construct containing the NF-κB *cis*-acting enhancer element. VSMCs and ECs were co-transfected with the reporter construct and alkaline phosphatase control plasmid (pSVAPAP). As expected the lowest NF-κB activity was detected in serum-starved ECs and VSMCs (Figures 7A and 7B). Compared with quiescent, in serum-stimulated VSMCs, the NF-κB reporter activity increased 4-fold, whereas NF-κB activity was not changed in ECs on serum stimulation. In contrast, TNF-α exposure of proliferating ECs and VSMCs led to 6- and 4.5-fold increases (versus quiescent), respectively, in NF-κB transcriptional activity (Figures 7A and 7B). However, in VSMCs overexpressing E2F1, NF-κB activation was completely abolished (Figure 7A), whereas NF-κB transcriptional activities were preserved in ECs under similar conditions (Figure 7B). These findings suggest a divergence in the signaling pathways triggered by overexpression of E2F1 in VSMCs versus ECs.

Discussion

Radiation therapy is currently available for inhibition of restenosis in stented arteries.[13] Although effective in reducing

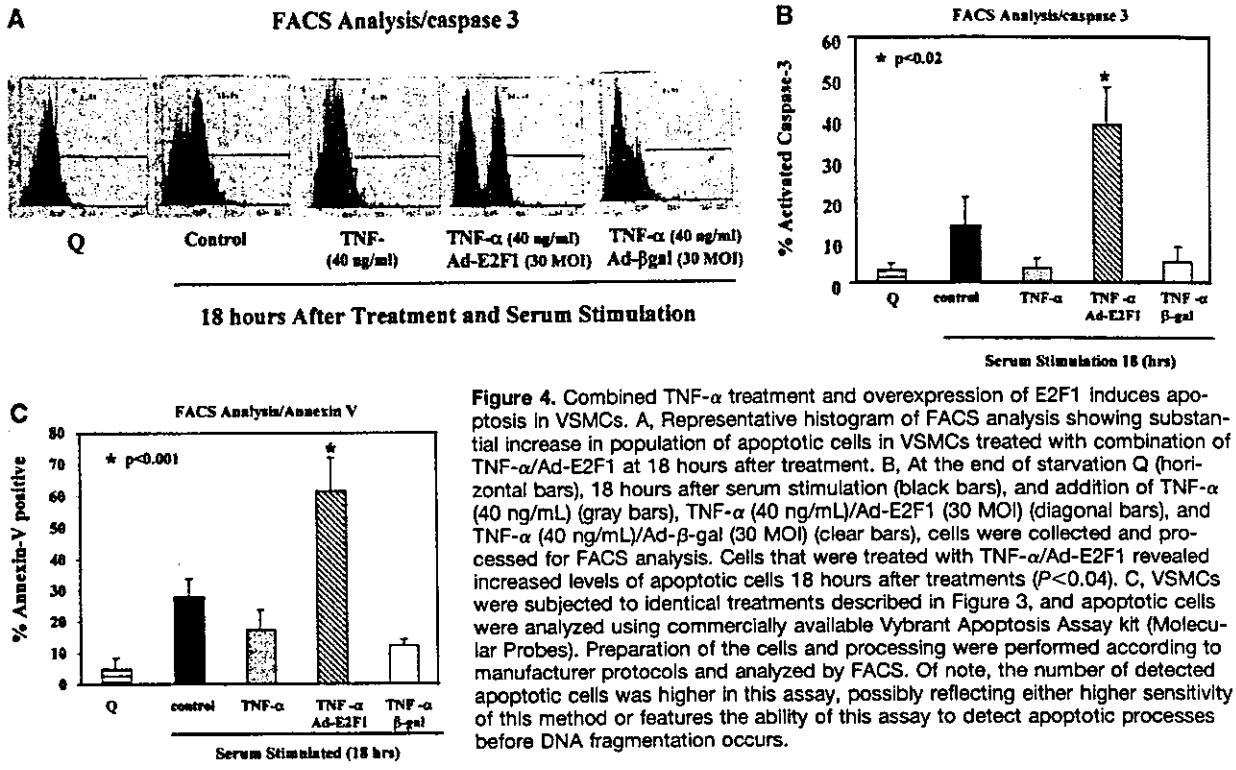

Figure 4. Combined TNF-α treatment and overexpression of E2F1 induces apoptosis in VSMCs. A, Representative histogram of FACS analysis showing substantial increase in population of apoptotic cells in VSMCs treated with combination of TNF-α/Ad-E2F1 at 18 hours after treatment. B, At the end of starvation Q (horizontal bars), 18 hours after serum stimulation (black bars), and addition of TNF-α (40 ng/mL) (gray bars), TNF-α (40 ng/mL)/Ad-E2F1 (30 MOI) (diagonal bars), and TNF-α (40 ng/mL)/Ad-β-gal (30 MOI) (clear bars), cells were collected and processed for FACS analysis. Cells that were treated with TNF-α/Ad-E2F1 revealed increased levels of apoptotic cells 18 hours after treatments ($P<0.04$). C, VSMCs were subjected to identical treatments described in Figure 3, and apoptotic cells were analyzed using commercially available Vybrant Apoptosis Assay kit (Molecular Probes). Preparation of the cells and processing were performed according to manufacturer protocols and analyzed by FACS. Of note, the number of detected apoptotic cells was higher in this assay, possibly reflecting either higher sensitivity of this method or features the ability of this assay to detect apoptotic processes before DNA fragmentation occurs.

the incidence of recurrent neointimal proliferation, this strategy is compromised by delayed reendothelialization,[14] which results in a significant incidence of late stent thrombosis.[13,15] More recently, a great deal of enthusiasm has been generated by reports that rapamycin and other cell cycle inhibitors are capable of eliminating restenosis.[16] Because this chemotherapy strategy shares with radiation therapy an approach that is not designed to enhance endothelial recovery, it would come as no surprise to learn of late events due to endothelial dysfunction. Indeed, recent reports indicate a distinct antiendothelial action of rapamycin.[17] In contrast to these prior strategies, the present studies suggest that, by exploiting certain signaling pathways in ECs and VSMCs, it may be possible to develop an approach to restenosis that is capable of inhibiting neointimal thickening while simultaneously encouraging recovery of a functional endothelium.

In response to vascular injury, proinflammatory cytokines, such as TNF-α, are produced by activated macrophages as well as by VSMCs themselves.[1] Locally released TNF-α can regulate gene expression, differentiation, growth, and apoptosis of ECs and VSMCs at sites of vascular injury.[1,18] The clinical relevance of TNF-α expressed at sites of balloon injury was documented in our earlier studies showing acceleration of reendothelialization in injured vessels after TNF-α soluble receptor-mediated blocking of TNF-α.[3] We have also previously shown that TNF-α inhibited E2F1 expression and activity in vitro, accompanied by cell cycle arrest and enhanced apoptosis in proliferating ECs.[2] Overexpression of E2F1 restored EC proliferation and inhibited apoptosis despite TNF-α exposure.[2] The present studies reveal that the in vitro survival effect of E2F1 on ECs translates in vivo into enhanced endothelial recovery at sites of balloon injury.

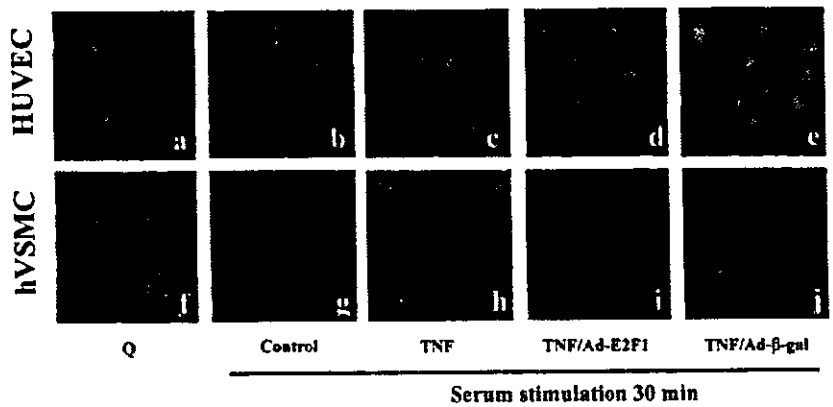

Figure 5. Immunofluorescent staining demonstrating nuclear translocation of NF-κB (p65) in VSMCs and HUVECs. VSMCs and HUVECs were subjected to identical treatments described in legend to Figure 3. Localization of NF-κB (p65) was determined by confocal microscopy. Cells were visualized using magnification of ×40. Similar results were obtained in two independent experiments.

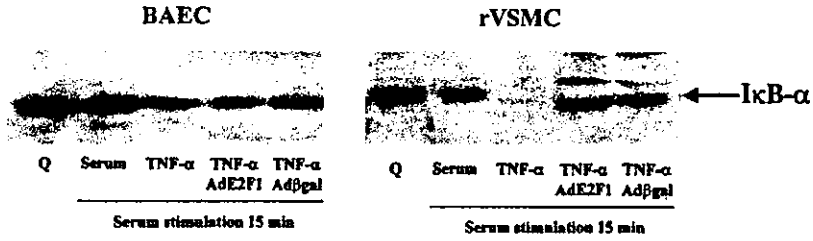

Figure 6. Inhibition of IkB-α degradation in VSMCs. Western blot analysis demonstrating inhibition of IkB-α degradation in VSMCs 15 minutes after serum stimulation and treatment with TNF-α/Ad-E2F1. In contrast, similar treatment of BAECs enhances IkB-α degradation.

Moreover, and perhaps more important, they document a divergence in the TNF-α/E2F1 signaling pathways of ECs and VSMCs under similar external cues. Instead of augmenting VSMC survival and proliferation as it did in ECs, E2F1 overexpression induces apoptosis and inhibits VSMC cell cycle progression. These findings thus identify a unique therapeutic approach: simultaneously targeting the cell cycle of two different cell types, within the same tissue microenvironment, via a pathway which results in opposite and biologically complimentary effects.

E2F1, a member of the E2F family of transcription factors plays a major role in regulating a diverse array of cellular functions including gene expression, proliferation, differentiation, and apoptosis.[19] These differential effects of E2F1, however, appear to be cell and stimulus specific.[20] Differential regulation of cell proliferation and apoptosis by deregulated E2F1 in ECs and VSMCs shown in this study is supported by other studies reporting similar desperate effects of E2F1 on these cellular functions in different cell types. Overexpression of E2F1 either promoted S-phase entry and proliferation[21] or apoptosis.[22,23] Our finding that overexpression of E2F1 enhances VSMC apoptosis is also in agreement with a recent study in which E2F1 induced caspase 3–like activity and initiated apoptosis in coronary VSMCs.[24] This study, however, differs from ours in the unique context of TNF-α exposure that mimics the in vivo arterial injury environment. Thus, our study demonstrates a negative, cooperative effect of TNF-α and E2F1 overexpression on VSMC proliferation and survival, because within the time frame of our experiments, TNF-α alone did not have a significant effect on VSMC survival. Additionally, no previous study has documented a biologically different response to TNF-α/E2F-1 by two neighboring cell types within the same tissue.

Transmembrane signaling after TNF-α receptor binding triggers cellular apoptosis in some cancer cells[25,26] and endothelial cells[27] yet induces proliferation in normal diploid fibroblasts.[25] Unresponsiveness of VSMCs to TNF-α seen in our study is supported by the evidence from other studies showing that TNF-α itself has little effect on the growth or apoptosis of VSMCs.[28] The conclusion that E2F1 overexpression–mediated apoptosis in VSMCs results from a synergistic effect of E2F1/TNF-α is further strengthened by the data showing a significant increase in the activation of caspase 3, a marker for apoptotic cells, in Ad-E2F1–transduced VSMCs exposed to TNF-α (Figures 4A and 4B).

TNF-α signaling involves activation of various secondary messengers[29] that in turn directly or indirectly lead to the activation of NF-κB, which then transcriptionally induces many genes.[26] NF-κB has been also implicated in atherosclerosis because activated NF-κB is present in atherosclerotic lesions[30] but not in normal tissues.[31] In addition, in the rat model of arterial injury, NF-κB activity was induced at the time of rapid proliferation of VSMCs and neointima formation after balloon angioplasty.[32] It is therefore conceivable that E2F1 overexpression–mediated inhibition of VSMC proliferation might reflect modulations in the NF-κB activity. Indeed, there is ample evidence suggesting E2F1-mediated inhibition of NF-κB and a consequential increase in apoptosis in various cell types.[23] Mechanisms proposed for this inhibition, however, remain unclear. Tanaka et al[23] showed that endogenous E2F1 competes with p50 for binding to p65 subunit of NF-κB and that this physical interaction of E2F1/p65 inhibits NF-κB transcriptional activities. It is noteworthy that VSMCs used in this study express almost undetectable level of endogenous E2F1 (Figure 3A). It is therefore not surprising that in TNF-α exposed, serum-stimulated VSMCs, we found no apparent apoptosis. Similarly E2F1 has also been shown to interact with p50 subunit of NF-κB in Jurkat cells.[33] Additionally, Phillips et al[9] have shown that in Saos2 cells, E2F1-induced inhibition of NF-κB activity was mediated by the abrogation of TRAF-2 protein and inhibition of IkB kinase. And finally, Yoshimura et al[34]

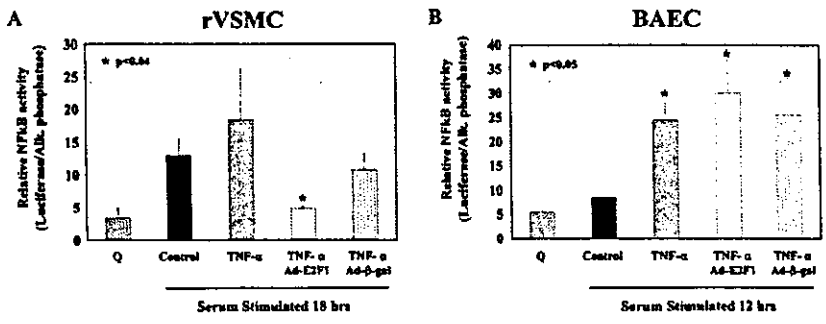

Figure 7. Overexpression of Ad-E2F1 inhibits NF-κB transcriptional activities in VSMCs. A, NF-κB activity was reduced by 68% to 78% ($P<0.04$) in combined TNF-α/AdE2F1–treated cells (open bars). Results represent mean±SD of triplicate dishes. Similar results were obtained in three independent experiments. B, After serum stimulation with or without TNF-α, BAECs were harvested at 12 hours after stimulation. In contrast to VSMCs, overexpression of E2F1 did not abrogate NF-κB transcriptional activity (open bars), which remained similar to TNF-α (gray bars) and/or TNF-α/Ad-β-gal (dotted bars)–treated BAECs ($P<0.05$). Results represent mean±SD of triplicate dishes.

have recently shown that NF-κB decoy inhibits neointimal formation in an animal model.

In the present study, we show that divergent E2F1 effects on TNF-α–exposed ECs and VSMCs exposed to TNF-α are, at least in part, dependent on cell-specific inhibition of NF-κB nuclear translocation and transcriptional activities in VSMCs. Inhibition of IkB-α degradation in VSMCs suggests that NF-κB remains sequestered in the cytoplasm; an observation that parallels the results obtained in nuclear translocation and promoter activity studies. However, signaling events upstream of IkB-α in E2F1/TNF-α–treated ECs and VSMCs leading to differential cellular response remain to be elucidated and are beyond the scope of this study. More detailed understanding of the mechanisms driving the cell cycle machinery in ECs versus VSMCs may yield important insights permitting the development of comprehensive therapies for restenosis prevention.

Acknowledgments

This study was supported in part by NIH grants (HL-53354, HL-60911, HL-63414, HL-63695, and HL-66957) and the Shaughnessy center for clinical genetics. This article is dedicated to Dr Jeffrey M. Isner who passed away on October 31, 2001. We would like to gratefully acknowledge his inspirational leadership. We gratefully acknowledge M. Neely and I. Johnson for their assistance in the preparation of this manuscript.

References

1. Warner SJ, Libby P. Human vascular smooth muscle cells: target for and source of tumor necrosis factor. *J Immunol.* 1989;142:100–109.
2. Spyridopoulos I, Principe N, Krasinski KL, Xu S, Kearney M, Magner M, Isner JM, Losordo DW. Restoration of E2F expression rescues vascular endothelial cells from tumor necrosis factor-α–induced apoptosis. *Circulation.* 1998;98:2883–2890.
3. Krasinski K, Spyridopoulos I, Kearney M, Losordo DW. In vivo blockade of tumor necrosis factor-α accelerates functional endothelial recovery after balloon angioplasty. *Circulation.* 2001;104:1754–1756.
4. Krasinski K, Asahara T, Spyridopoulos I, Isner JM, Losordo DW. Estradiol accelerates endothelial recovery after arterial injury. *Circulation.* 1997;95:1768–1772.
5. Perlman H, Luo Z, Krasinski K, Le Roux A, Mahfoudi A, Smith RC, Branellec D, Walsh K. Adenovirus-mediated delivery of the Gax transcription factor to rat carotid arteries inhibits smooth muscle proliferation and induces apoptosis. *Gene Ther.* 1999;6:758–763.
6. Lindner V, Fingerle J, Reidy MA. Mouse model of arterial injury. *Circ Res.* 1993;73:792–796.
7. Spyridopoulos I, Sullivan AB, Kearney M, Isner JM, Losordo DW. Estrogen-receptor-mediated inhibition of human endothelial cell apoptosis: estradiol as a survival factor. *Circulation.* 1997;95:1505–1514.
8. Stiewe T, Putzer BM. Role of the p53-homologue p73 in E2F1-induced apoptosis. *Nat Genet.* 2000;26:464–469.
9. Phillips AC, Ernst MK, Bates S, Rice NR, Vousden KH. E2F-1 potentiates cell death by blocking antiapoptotic signaling pathways. *Mol Cell.* 1999;4:771–781.
10. Mayo MW, Wang CY, Cogswell PC, Rogers-Graham KS, Lowe SW, Der CJ, Baldwin AS Jr. Requirement of NF-κB activation to suppress p53-independent apoptosis induced by oncogenic Ras. *Science.* 1997;278:1812–1815.
11. Madrid LV, Wang CY, Guttridge DC, Schottelius AJ, Baldwin AS Jr, Mayo MW. Akt suppresses apoptosis by stimulating the transactivation potential of the RelA/p65 subunit of NF-κB. *Mol Cell Biol.* 2000;20:1626–1638.
12. Perlman H, Maillard L, Krasinski K, Walsh K. Evidence for the rapid onset of apoptosis in medial smooth muscle cells after balloon injury. *Circulation.* 1997;95:981–987.
13. Waksman RBB, Mintz GS, Mehran R, Lansky AJ, Satler LF, Kent KM, Leon MB. Late total occlusion after intracoronary brachytherapy for patients with in-stent restenosis. *J Am Coll Cardiol.* 2000;36:65–68.
14. Farb A, Shroff S, John M, Sweet W, Virmani R. Late arterial responses (6 and 12 months) after ^{32}P β-emitting stent placement: sustained intimal suppression with incomplete healing. *Circulation.* 2001;103:1912–1919.
15. Leon MB, Teirstein PS, Moses JW, Tripuraneni P, Lansky AJ, Jani S, Wong SC, Fish D, Ellis S, Holmes DR, Kerieakes D, Kuntz RE. Localized intracoronary gamma-radiation therapy to inhibit the recurrence of restenosis after stenting. *N Engl J Med.* 2001;344:250–256.
16. Morice MC, Serruys PW, Sousa JE, Fajadet J, Ban Hayashi E, Perin M, Colombo A, Schuler G, Barragan P, Guagliumi G, Molnar F, Falotico R. A randomized comparison of a sirolimus-eluting stent with a standard stent for coronary revascularization. *N Engl J Med.* 2002;346:1773–1780.
17. Guba M, von Breitenbuch P, Steinbauer M, Koehl G, Flegel S, Hornung M, Bruns CJ, Zuelke C, Farkas S, Anthuber M, Jauch KW, Geissler EK. Rapamycin inhibits primary and metastatic tumor growth by antiangiogenesis: involvement of vascular endothelial growth factor. *Nat Med.* 2002;8:128–135.
18. Lin J, Liliensiek B, Kanitz M, Schimanski U, Bohrer H, Waldherr R, Martin E, Kauffmann G, Ziegler R, Nawroth PP. Molecular cloning of genes differentially regulated by TNF-α in bovine aortic endothelial cells, fibroblasts and smooth muscle cells. *Cardiovasc Res.* 1998;38:802–813.
19. Field SJ, Tsai FY, Kuo F, Zubiaga AM, Kaelin WG Jr, Livingston DM, Orkin SH, Greenberg ME. E2F-1 functions in mice to promote apoptosis and suppress proliferation. *Cell.* 1996;85:549–561.
20. Nevins JR. Toward an understanding of the functional complexity of the E2F and retinoblastoma families. *Cell Growth Differ.* 1998;9:585–593.
21. Johnson DG, Schwarz JK, Cress WD, Nevins JR. Expression of transcription factor E2F1 induces quiescent cells to enter S phase. *Nature.* 1993;365:349–352.
22. Shan B, Lee WH. Deregulated expression of E2F-1 induces S-phase entry and leads to apoptosis. *Mol Cell Biol.* 1994;14:8166–8173.
23. Tanaka H, Matsumura I, Ezoe S, Satoh Y, Sakamaki T, Albanese C, Machii T, Pestell RG, Kanakura Y. E2F1 and c-Myc potentiate apoptosis through inhibition of NF-κB activity that facilitates MnSOD-mediated ROS elimination. *Mol Cell.* 2002;9:1017–1029.
24. Shelat HS, Liu TJ, Hickman-Bick DL, Barnhart MK, Vida T, Dillard PM, Willerson JT, Zoldhelyi P. Growth suppression of human coronary vascular smooth muscle cells by gene transfer of the transcription factor E2F-1. *Circulation.* 2001;103:407–414.
25. Sugarman BJ, Aggarwal BB, Hass PE, Figari IS, Palladino MA Jr, Shepard HM. Recombinant human tumor necrosis factor-α: effects on proliferation of normal and transformed cells in vitro. *Science.* 1985;230:943–945.
26. Wang C-Y, Mayo MW, Baldwin AS Jr. TNF- and cancer therapy-induced apoptosis: potentiation by inhibition of NF-κB. *Science.* 1996;274:784–787.
27. Spyridopoulos I, Brogi E, Kearney M, Sullivan AB, Cetrulo C, Isner JM, Losordo DW. Vascular endothelial growth factor inhibits endothelial cell apoptosis induced by tumor necrosis factor-α: balance between growth and death signals. *J Mol Cell Cardiol.* 1997;29:1321–1330.
28. Geng YJ, Wu Q, Muszynski M, Hansson GK, Libby P. Apoptosis of vascular smooth muscle cells induced by in vitro stimulation with interferon-γ, tumor necrosis factor-α, and interleukin-1β. *Arterioscler Thromb Vasc Biol.* 1996;16:19–27.
29. Berk BC, Abe JI, Min W, Surapisitchat J, Yan C. Endothelial atheroprotective and anti-inflammatory mechanisms. *Ann N Y Acad Sci.* 2001;947:93–109; discussion 109–111.
30. Brand K, Page S, Rogler G, Bartsch A, Brandl R, Knuechel R, Page M, Kaltschmidt C, Baeuerle PA, Neumeir D. Activated transcription factor nuclear factor-κB is present in the atherosclerotic lesion. *J Clin Invest.* 1996;97:1715–1722.
31. Bourcier T, Sukhova G, Libby P. The nuclear factor-κB signaling pathway participates in dysregulation of vascular smooth muscle cells in vitro and in human atherosclerosis. *J Biol Chem.* 1997;20:15817–15824.
32. Landry DB, Couper LL, Bryant SR, Lindner V. Activation of NK-κB and IκB system in smooth muscle cells after rat arterial injury: induction of vascular cell adhesion molecular-1 and monocyte chemoattractant protein-1. *Am J Pathol.* 1997;151:1085–1095.
33. Kundu M, Guermah M, Roeder RG, Amini S, Khalili K. Interaction between cell cycle regulator, E2F-1, and NF-κB mediates repression of HIV-1 gene transcription. *J Biol Chem.* 1997;272:29468–29474.
34. Yoshimura S, Morishita R, Hayashi K, Yamamoto K, Nakagami H, Kaneda Y, Sakai N, Ogihara T. Inhibition of intimal hyperplasia after balloon injury in rat carotid artery model using cis-element "decoy" of nuclear factor-κB binding site as a novel molecular strategy. *Gene Ther.* 2001;8:1635–1642.

Stromal Cell–Derived Factor-1 Effects on Ex Vivo Expanded Endothelial Progenitor Cell Recruitment for Ischemic Neovascularization

Jun-ichi Yamaguchi, MD, PhD; Kengo Fukushima Kusano, MD, PhD; Osamu Masuo, MD; Atsuhiko Kawamoto, MD, PhD; Marcy Silver, BS; Satoshi Murasawa, MD, PhD; Marta Bosch-Marce, PhD; Haruchika Masuda, MD, PhD; Douglas W. Losordo, MD; Jeffrey M. Isner, MD†; Takayuki Asahara, MD, PhD

Background—Stromal cell–derived factor-1 (SDF-1) is a chemokine considered to play an important role in the trafficking of hematopoietic stem cells. Given the close relationship between hematopoietic stem cells and endothelial progenitor cells (EPCs), we investigated the effect of SDF-1 on EPC-mediated vasculogenesis.

Methods and Results—Flow cytometric analysis demonstrated expression of CXCR4, the receptor of SDF-1, by 66±3% of EPCs after 7 days in culture. In vitro modified Boyden chamber assay showed a dose-dependent EPC migration toward SDF-1 (control versus 10 ng/mL SDF-1 versus 100 ng/mL SDF-1, 24±2 versus 71±3 versus 140±6 cells/mm^2; $P<0.0001$). SDF-1 attenuated EPC apoptosis (control versus SDF-1, 27±1 versus 7±1%; $P<0.0001$). To investigate the effect of SDF-1 in vivo, we locally injected SDF-1 into athymic ischemic hindlimb muscle of nude mice combined with human EPC transplantation to determine whether SDF-1 augmented EPC-induced vasculogenesis. Fluorescence microscopic examination disclosed increased local accumulation of fluorescence-labeled EPCs in ischemic muscle in the SDF-1 treatment group (control versus SDF-1=241±25 versus 445±24 cells/mm^2, $P<0.0001$). At day 28 after treatment, ischemic tissue perfusion was improved in the SDF-1 group and capillary density was also increased. (control versus SDF-1, 355±26 versus 551±30 cells/mm^2; $P<0.0001$).

Conclusion—These findings indicate that locally delivered SDF-1 augments vasculogenesis and subsequently contributes to ischemic neovascularization in vivo by augmenting EPC recruitment in ischemic tissues. (***Circulation.* 2003;107: 1322-1328.**)

Key Words: chemokines ■ angiogenesis ■ ischemia ■ endothelium

Stromal cell–derived factor-1 (SDF-1) is a member of the chemokine CXC subfamily originally isolated from murine bone marrow stromal cells.[1] It has a single substantial open reading frame of 267 nucleotides encoding an 89-amino acid polypeptide and expressed on stromal cells of various tissues. On the other hand, CXCR4, a 7-transmembrane-spanning G protein–coupled receptor, is the only known receptor for SDF-1 and is also a coreceptor for HIV type 1 infection.[2] SDF-1/CXCR4 interaction is reported to play an important physiological role during embryogenesis in hematopoiesis,[3] vascular development, cardiogenesis,[4] and cerebellar development.[5]

Recently, several investigators reported that CD34$^+$ cells, classically considered to be hematopoietic stem cells, expressed CXCR4, and that SDF-1 could induce CD34$^+$ cell migration in vitro.[6] Accordingly, SDF-1 is considered as one of the key regulators of hematopoietic stem cell trafficking between the peripheral circulation and bone marrow. SDF-1 has also been shown to effect CD34$^+$ cell proliferation[7] and mobilization[8] and to induce angiogenesis in vivo.[9]

Bone marrow–derived endothelial progenitor cells (EPCs) have been isolated from the peripheral blood of adult species.[10,11] These cells participate in not only physiological but also pathological neovascularization in response to certain cytokines and/or tissue ischemia.[12–14] More recently, ex vivo expanded EPCs from peripheral blood, transplanted into animal models of ischemic hindlimbs and acute myocardial infarction, successfully augmented neovascularization resulting in physiological recovery documented as limb salvage and improvement in myocardial function.[15,16]

Received August 12, 2002; revision received December 5, 2002; accepted December 5, 2002.

From the Division of Cardiovascular Research and Medicine (J.Y., K.F.K., O.M., A.K., M.S., S.M., M.B.M., D.W.L., J.M.I., T.A.), St Elizabeth's Medical Center, Tufts University School of Medicine, Boston, Mass, and Department of Physiology (H.M., T.A.), Tokai University School of Medicine, Tokai, Japan.

†Deceased.

Correspondence to Takayuki Asahara, MD, PhD, or Douglas W. Losordo, MD, Division of Cardiovascular Research and Medicine, St Elizabeth's Medical Center, 736 Cambridge St, Boston, MA, 02135. E-mail asa777@aol.com (T.A.) or douglas.losordo@tufts.edu

Circulation is available at http://www.circulationaha.org

DOI: 10.1161/01.CIR.0000055313.77510.22

At present, however, enthusiasm for the therapeutic potential of strategies of EPC transplantation is limited by certain practical considerations. For example, adjusting the number of EPCs for injection according to body weight, ≈6 L of blood would be required for harvesting of EPCs in an average-size patient to administer a dose equivalent to that which yielded therapeutic effects in limb and myocardial ischemia in small animal models. Accordingly, we investigated the hypothesis that locally administered SDF-1 could augment the local accumulation of transplanted EPCs, thereby resulting in enhanced neovascularization. Here we report that EPCs express CXCR4 and that the combination of SDF-1 local administration and EPC transplantation has potential as a strategy for therapeutic neovascularization.

Methods

Cell Isolation and Culture

Ex vivo expansion of EPCs was performed as described.[10] In brief, total human peripheral blood mononuclear cells were isolated from healthy human volunteers by density-gradient centrifugation with Histopaque-1077 (Sigma) and plated on culture dishes coated with human fibronectin (Sigma). The cells were cultured in endothelial cell basal medium-2 (EBM-2, Clonetics) supplemented with 5% FBS, human vascular endothelial growth factor (VEGF)-A, human fibroblast growth factor-2, human epidermal growth factor, insulin-like growth factor-1, ascorbic acid, and antibiotics. After 4 days in culture, nonadherent cells were removed by washing with PBS, new medium was applied, and the culture was maintained through day 7.

$CD34^+$ cells from isolated human peripheral blood mononuclear cells were positively selected using the MiniMACS immunomagnetic separation system (Milteney Biotec) according to the manufacturer's instructions as recently described.[7]

Fluorescence-Activated Cell Sorting

Fluorescence-activated cell sorting (FACS) detection of EPCs was performed after 7 days in culture. The procedure of FACS staining was described previously.[16] In brief, a total of 2 to 3×10^5 cells were resuspended with 200 μL of Dulbecco's PBS (BioWhittaker) containing 10% FBS and 0.01% NaN_3 and incubated for 20 minutes at 4°C with phycoerythrin-conjugated monoclonal antibodies against CXCR4 (PharMingen). After staining, the cells were fixed in 2% paraformaldehyde. Quantitative FACS was performed on a FACStar flow cytometer (Becton Dickinson). All groups were studied at least in triplicate.

Migration Assay

To investigate EPC migration activity, a modified Boyden chamber assay was performed using a 48-well microchemotaxis chamber (NeuroProbe) as described.[17] In brief, SDF-1 (PharMingen) is diluted to appropriate concentrations in EBM-2 supplemented with 0.1% BSA, and 30 μL of the final dilution was placed in the lower compartment of a Boyden chamber. Human EPCs cultured for 7 days were harvested, 3×10^4 cells were suspended in 50 μL of EBM-2 supplemented with 0.1% BSA, and antibiotics were reseeded in the upper compartment. After incubation for 5 hours at 37°C, the filter was removed, and the cells on the filter were counted manually in random high-power fields (×100) in each well. All groups were studied at least in triplicate.

Apoptosis Assay

EPC apoptosis, induced by serum starvation, was quantified to determine whether SDF-1 exerts a survival effect on EPCs. The proportion of apoptotic EPCs after serum starvation was determined by manually counting pyknotic nuclei after DAPI (Roche) staining. In brief, day 7 EPCs were reseeded onto 4-chamber slides (1×10^5 cells per well with 500 μL of EPC culture medium). After 24 hours of incubation, culture medium was removed and replaced with 500 μL of EBM-2 without any supplement. After 48 hours of serum deprivation, the medium was supplemented with 100 ng/mL of SDF-1 (versus medium alone) and incubated for 3 hours. DAPI-stained pyknotic nuclei were counted as percentage of 100 cells in each well. Each group was studied at least in triplicate.

Animal Model of Ischemic Hindlimb

All procedures were performed in accordance with the Institutional Animal Care and Use Committee of St Elizabeth's Medical Center. Male athymic nude mice (CBy-Cg-Foxn1^{nu}, The Jackson Laboratory), age 8 to 10 weeks and weighing 18 to 22 g, were anesthetized with sodium pentobarbital (160 mg/kg IP) for operative resection of one femoral artery as described.[16] For euthanization, mice were injected with an overdose of pentobarbital.

RNA Extraction and Reverse Transcriptase–Polymerase Chain Reaction Analysis

Tissue RNA was extracted from frozen muscle samples (day 7 after hindlimb ischemia) using TRIzol reagent (Invitrogen) according to the manufacturer's instructions. Reverse transcriptase–polymerase chain reaction (RT-PCR) of the VEGF and GAPDH genes was performed using 1 μg of total RNA. PCR was performed for 35 cycles for VEGF-A and 25 cycles for GAPDH, with each cycle consisting of 94°C for 30 seconds and 64°C for 3 minutes. Amplification was carried out in 20-μL reaction mixtures containing 0.4 U *Taq* polymerase.

Transplantation of Ex Vivo Expanded EPCs

The impact of local administration of SDF-1 after EPC transplantation on therapeutic neovascularization was investigated in a murine model of hindlimb ischemia.[16] Just after operative excision of one femoral artery, athymic nude mice, described above, in which angiogenesis is characteristically impaired, received a local intramuscular injection of 1 μg SDF-1 versus PBS in the center of the lower calf muscle followed immediately by an intravenous injection of 1.5×10^5 culture-expanded EPCs. To evaluate EPC incorporation into the vasculature in ischemic muscles, some mice were transplanted with EPCs labeled with the fluorescent carbocyanine 1,1′-dioctadecyl-1 to 3,3,3′3′-tetramethylidocarboyanine perchlorate (DiI) dye (Molecular Probes). Before transplantation, EPCs in suspension were washed with PBS and incubated with DiI at a concentration of 2.5 μg/mL PBS for 5 minutes at 37°C and 15 minutes at 4°C. After 2 washing steps in PBS, the cells were resuspended in EBM-2. Five mice in the placebo and SDF-1 groups each received 1.5×10^5 DiI-labeled EPCs intravenously as described above. Thirty minutes before euthanization at day 3 and day 7, 5 mice in each group received an intravenous injection of 50 μg of *Bandeiraea simplicifolia* lectin 1 (BS-1 lectin, Vector Laboratories) to identify the mouse vasculature.

Physiological Assessment of Transplanted Animals

Laser Doppler perfusion imaging (LDPI, Moor Instruments) was used to record serial blood flow measurements over the course of 4 weeks postoperatively, as previously described.[16] There were 8 mice in the SDF-1 group and 9 in the PBS group. In these digital color-coded images, a red hue indicates the region of maximum perfusion, medium perfusion values are shown in yellow, and the lowest perfusion values are represented by blue. Figure 5B displays absolute values in readable units.

Histological Assessment of Transplanted Animals

Tissue sections from the lower calf muscles of ischemic and healthy limbs were harvested on days 3, 7, and 28. To examine EPC incorporation at early time points after transplantation (at days 3 and 7) and SDF-1 effect on host endothelial cells, tissues from the mice injected with DiI-labeled EPCs and BS-1 lectin were embedded for frozen section samples. A total of 20 different fields (4 cross sections from each animal) were randomly selected, and the DiI-labeled EPCs were counted (×40 magnification).